Carbohydrate Secondary and Tertiary Structure Using Raman Spectroscopy

40

Shaun Thomas Mutter and Ewan William Blanch

Contents

Abstract

Raman spectroscopy is a long-established analytical technique that has now proliferated into a variety of research tools that are able to identify and characterize almost any type of molecule under most conditions. As such, Raman spectroscopies are well suited to the study of carbohydrates, from simple monosaccharides to the largest glycosaminoglycans and from industrial bioreactors to *in situ* measurements on living cells. This review covers a range of examples of how Raman techniques are addressing the questions of glycobiologists working on diverse aspects of this fascinating but poorly understood class of biomolecules.

S.T. Mutter
Manchester Institute of Biotechnology and Faculty of Life Sciences, The University of Manchester, Manchester, UK
e-mail: shaun.mutter@manchester.ac.uk

E.W. Blanch (✉)
School of Applied Sciences, RMIT University, Melbourne, VIC, Australia
e-mail: e.blanch@manchester.ac.uk

K.G. Ramawat, J.-M. Mérillon (eds.), *Polysaccharides*,
DOI 10.1007/978-3-319-16298-0_36

Focus is placed on the application of Raman, surface-enhanced Raman, Raman optical activity, and related spectroscopies to characterizing carbohydrates of all types, with only a general introduction to the theory of the techniques themselves. Particular attention is also paid to the computational tools now regularly used by spectroscopists to analyze complex data. Although this review is aimed at the glycobiology community, the examples discussed also demonstrate to the expert spectroscopist how their techniques can impact on the exciting opportunities presented by working with carbohydrates.

1 Introduction

While the importance of carbohydrates to both the natural world and human society is clear, it is surprising how limited is our current understanding of the structural parameters that control the function and behavior of complex carbohydrates, particularly in contrast to proteins and DNA which are far better understood. While high-resolution structural techniques such as X-ray crystallography and nuclear magnetic resonance (NMR) have revolutionized biology through their ability to reveal detailed information on proteins and nucleic acids, they are less applicable to carbohydrates. Most glycoproteins and polysaccharides do not form diffractable crystals, while their typical combination of large size and low sequence complexity often prevents the acquisition of well-resolved NMR spectra. The development of our understanding of how sugars, glycans, and polysaccharides behave therefore requires the use of other biophysical techniques.

Raman spectroscopy, which measures the vibrational motions of molecules induced through the inelastic scattering of light, possesses several characteristics that makes it particularly suitable as an analytical technique for carbohydrates. Raman spectra can be obtained from samples in any physical state, which is particularly significant considering that complex carbohydrates are commonly found in solution, solid, and gel states; the technique is noninvasive and nondestructive; there is no size limit to the samples that can be studied, allowing studies on high molecular weight polysaccharides and large glycoproteins; and the spectra contain information about all levels of biomolecular structure. There are also a number of variants of conventional Raman spectroscopy that have been used to provide important new insights into carbohydrate structure. Surface-enhanced Raman scattering (SERS) exhibits a significant boosting of Raman bands due to surface plasmons generated by specific metal surfaces, thereby increasing sensitivity to even trace levels of biomolecules and forming the basis for a new generation of biosensors. Raman optical activity (ROA) is the chirally sensitive form of Raman scattering and displays an exquisite sensitivity to stereochemistry and conformational dynamics. These complementary Raman techniques together form a valuable toolkit for glycobiology, and this review presents an introduction to each of these methods and examples of their application to carbohydrates. We also discuss the capabilities of density functional theory (DFT) modeling and chemometrics for revealing further structural information about carbohydrates from these spectra.

The purpose of this review is not to exhaustively cover all previous research in this field but to illustrate to glycobiologists, through the use of relevant examples, how different Raman techniques can generate new information on carbohydrates and their behavior.

1.1 Raman Spectroscopy

Photons interact with matter in a number of ways including through absorbance and reflection. A proportion of photons will be scattered from molecules, and most of these elastically scatter, with no energy transfer, which is called Rayleigh scattering. However, a small proportion of the scattered photons (around 10^{-7} of the incident photons) will undergo a transfer of energy, either from the photon to the molecule, so raising it to an excited vibrational state (Stokes scattering), or from a molecule in an excited vibrational state to the photon, thus returning it to a lower energetic state (anti-Stokes scattering). In Raman spectroscopy, monochromatic radiation is used to excite Raman scattering, and, most typically, the Stokes-scattered photons are collected and analyzed as this leads to the optimum signal intensity as Boltzmann averaging dictates that there are more molecules in the ground vibrational state than in excited states. The differences in energy between the Raman-scattered and incident photons will correspond to vibrational motions of the molecule, which depend upon the atoms involved in the vibrational mode and their local environments. There are 3n–6 vibrational modes of a nonlinear molecule (where n is the number of atoms), with many, or most, of these potentially giving rise to Raman transitions. Therefore, the Raman spectrum of any molecule is an information-rich fingerprint of the molecule and any structural changes induced by the experimental conditions, e.g., through changes in temperature, pH, and binding interactions, or any other chemical or physical factor. Many different types of Raman spectrometer can be found, with these being optimized for different purposes, with Raman microscopes being particularly popular for studies on solids, including cells and tissues. For biological samples, care may have to be exercised in selecting the most appropriate type of Raman instrument. This is particularly true in terms of the competing factors of scattering efficiency, which is related to the excitation wavelength (λ) by λ^{-4} and so is higher at shorter wavelengths, and fluorescence, which can overwhelm a Raman spectrum and is more intense at shorter visible wavelengths. In the case of pure samples of carbohydrates, fluorescence is not typically a serious problem; however, for biofluids and tissues, this may be an issue.

A typical Raman spectrum of a simple carbohydrate is shown in Fig. 1, in this case for D-ribose in water at ~20 °C. Characteristic band patterns related to the functional groups of the saccharide are evident over the presented range of 300–1,800 cm^{-1}. Although they are not shown in this figure, other spectral regions can also be studied, particularly the C–H stretching region from ~2,800 to 3,100 cm^{-1}, N–H stretching region from ~3,200 to 3,600 cm^{-1}, with O–H stretching modes usually appearing ~3,600–3,700 cm^{-1}, and carboxylic acids

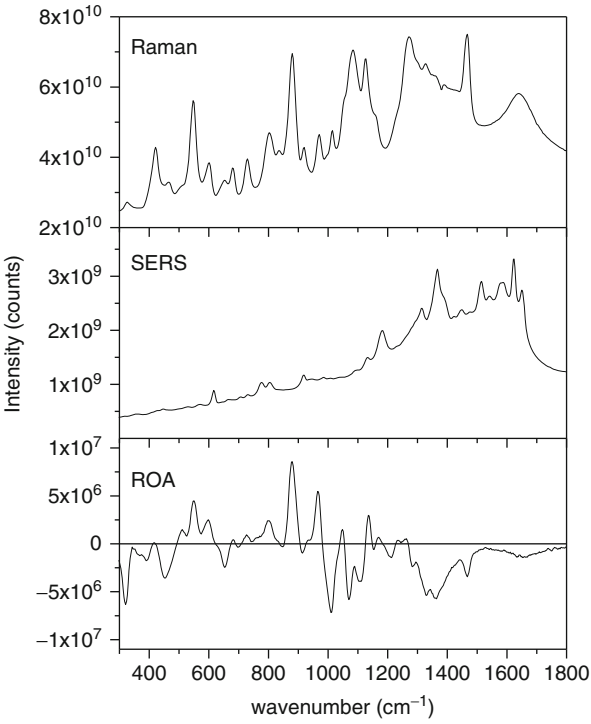

Fig. 1 Raman (*top*), SERS (*middle*), and ROA (*bottom*) spectra of D-ribose in solution. The Raman and ROA spectra were recorded at a concentration of 2.66 M for 237 min and with laser power at the sample of 625 mW. The SERS spectrum of D-ribose was measured with a concentration of 1.67 mM, for 20 min with 100 mW laser power. For the SERS measurement, silver citrate-reduced colloids and 20 mM K_2SO_4 as the aggregating agent were used (Figure was adapted from Ostovar Pour et al. 2011)

generating additional bands between 2,500 and 3,200 cm^{-1}. Detailed analysis of the functional group origins of these Raman bands can be found elsewhere (Ostovar pour et al. 2011), but in general many of the Raman modes of sugars over this range tend to involve complex combinations of molecular vibrations, with many of the Raman bands presented here for D-ribose from 700 to 1,100 cm^{-1} originating from various C–C and C–O stretching motions, sometimes with coupling to O–H deformations. Raman bands of carbohydrates from 1,300 to 1,600 cm^{-1} generally arise from CH deformations, and below 700 cm^{-1} can be seen bands signifying deformation modes of the skeletal ring backbone. The anomeric ratio can also be directly characterized from Raman bands in the region of ~630–700 cm^{-1} (Mathlouthi et al. 1983; Carmona and Molina 1990). The complex band patterns of carbohydrate Raman spectra make them useful fingerprints of identity and functional group composition, as well as the effects on structure induced by the local environment.

1.2 Surface-Enhanced Raman Scattering (SERS)

Although Raman spectroscopy is now widely used in the chemical, biological, and even medical sciences, it still is generally viewed as a relatively weak effect. One solution to this problem is the use of plasmon resonance enhancement mechanisms to greatly reduce detection limits and increase spectral intensities, which leads to

surface-enhanced Raman scattering (SERS). There are many detailed reviews on the origin and potential applications of SERS (Anker et al. 2008; Schlucker 2009, 2014; McNay et al. 2011; Larmour and Graham 2011; Kitahama et al. 2012; Ringe et al. 2013; Yamamoto et al. 2014), and so we present only a brief summary here of the relevant aspects.

While the first observation of SERS, of pyridine on an electrochemically roughened silver surface, was made by Fleischmann et al. (1974), it was in 1977 that two other groups suggested mechanisms for the enhancement process that are today widely accepted as being correct (Jeanmaire and van Duyne 1977; Albrecht and Creighton 1977). Considerable debate has been generated on the relative importance of different contributing factors to the SERS effect, but it is generally recognized that there are two main effects involved. The electromagnetic (EM) mechanism describes how an incident light wave can excite localized surface plasmons in the vicinity of roughened or geometric features on the surface of certain metals, with the most commonly used being silver or gold. The greatly enhanced local electric field then leads to an increase in Raman intensity. Both the Raman incident and emitted fields may be enhanced, generally by different amounts. The nature of the metal surface will affect the plasmon resonance frequency, so changing the SERS response. In general, silver surfaces give strongest enhancements for visible excitation frequencies, while gold surfaces work best at near-infrared excitation frequencies.

Although the EM mechanism is thought to be responsible for much of the observed SERS spectrum, it does not explain the whole process, and an additional contribution comes from the chemical enhancement (CE) mechanism. The CE mechanism involves charge transfer between the chemisorbed analyte molecule and the metal surface. It can be generalized that while the EM mechanism is responsible for most of the signal enhancement observed, the CE mechanism gives rise to the selective band enhancement that makes the SERS spectrum distinctive and different to the parent Raman spectrum. In Fig. 1, the SERS spectrum of D-ribose clearly has a different profile to the corresponding Raman spectrum due to the chemical enhancement of selected Raman bands. Although establishing the molecular origins of SERS bands is a subject of ongoing research for many group, most SERS bands measured for carbohydrates are not yet assigned in the literature. These SERS spectra are therefore commonly used as spectral fingerprints for the detection of specific sugars under conditions of low concentration and laser power. We note that the principal bands shown in the SERS spectrum for D-ribose are between 4 and 5 orders of magnitude stronger than the corresponding Raman features, on a per molecule basis. Such enhancement factors are commonly obtained, verifying the sensitivity of SERS as a bioanalytical tool.

1.3 Raman Optical Activity (ROA)

Raman optical activity (ROA) measures a small difference in the intensity of Raman scattering from chiral molecules using right- and left-circularly polarized

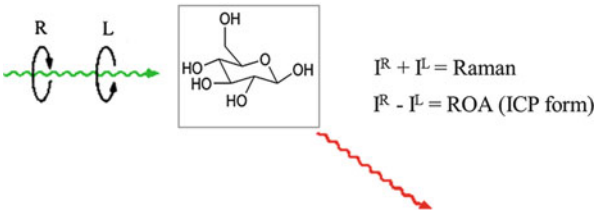

Fig. 2 Schematic of the ROA scattering process, specifically showing the incident circular polarization (*ICP*) form. If the scattered radiation was circularly polarized instead, this would correspond to the SCP form. The SCP form is most widely used, but in the absence of resonance effects, the ICP and SCP forms are equivalent and generate the same spectra (Figure is adapted from Barron et al. 2000)

light; see Fig. 2. ROA was first predicted in 1969 by Atkins and Barron (1969) and then observed experimentally in 1972 by Barron et al. (1973). Until recently, ROA spectroscopy was only used in a handful of laboratories around the world as it is a weak effect which requires careful measurement, with ROA scattering intensities typically being 10^{-3} to 10^{-5} of the corresponding Raman scattering. Although still a niche technique, at the time of writing, ROA was now available in around 30 laboratories globally, in both universities and pharmaceutical companies.

As is shown in Fig. 2, the circular polarization may be in either the incident light, leading to incident circular polarization (ICP) ROA, or the scattered light, leading to scattered circular polarization (SCP) ROA, or even in both, which gives rise to dual circular polarization (DCP) ROA. Most early ROA measurements, until around 2004, were made with the ICP form, but since then SCP ROA is the most common. However, this does not present a problem for comparing spectra measured with the different forms of ROA as in the far-from-resonance limit they give the same spectra. As can be clearly seen in Fig. 1, as ROA is a difference measurement, the spectrum is bisignate, with both positive and negative features. The ROA bands observed originate from the Raman bands, but as ROA spectral features derive from not only the electric polarizability but also the magnetic polarizability and the quadruple moment, ROA features display different intensities and bandshapes to the corresponding Raman features. They can also present both mono- and bisignate features. This is apparent for several of the ROA bands of D-ribose, shown in Fig. 1. Further details of the sensitivity of ROA bands to the local stereochemistry and structure of carbohydrates are discussed in this review, below.

The ROA measurement can be represented quantitatively by the circular intensity difference (CID), defined as:

$$\Delta = \left(I^R - I^L\right)/\left(I^R + I^L\right) \tag{1}$$

where I^R and I^L are the scattered Raman intensities in right- and left-circularly polarized incident light, respectively. If the R and L labels were subscripted, this would denote right- and left-circularly polarized scattered light intensities. As was mentioned above, in the absence of electronic enhancement, which is the typical

case for ROA studies on carbohydrates, the incident and scattered CID expressions are equivalent. For readers interested in the theory of ROA or its general application to other classes of molecules, we recommend any of several comprehensive reviews (Blanch et al. 2003; Barron et al. 2003, 2004; Barron and Blanch 2009).

2 Studies on Simple Carbohydrates

Early Raman studies on mono-, oligo-, and polysaccharides were mainly conducted on crystalline samples; see, e.g., Cael et al. (1974), Mathlouthi and Koenig (1986), Wells and Atalla (1990), and Dauchez et al. (1994a, b). These studies established that many of the vibrational modes of monosaccharides are complex and involve greater mixing of internal coordinates than is generally found for peptides and amino acids. Although this can make detailed analysis of the vibrational modes of sugars more challenging than for other biological molecules, the results from these studies indicated that characteristic spectral fingerprints could still be identified. Thus, the ability of Raman spectroscopy to differentiate between different monosaccharides, and so serve as a sensitive probe of carbohydrate identity, has been known for some time. Kačuráková and Mathlouthi (1996) found that they could use the Raman profiles to distinguish between a selection of simple sugars (D-glucose, D-galactose, lactose, maltose, melibiose, maltotriose, raffinose, and trehalose) in solution. These authors also found that distinctive Raman bands of the monosaccharides could be detected in the spectra of several of the disaccharides as the conformations of the individual sugars were very similar to those of the corresponding subunits. This contrasted with the larger changes observed in the spectra of melibiose and trehalose, as a result of the larger structural differences induced by formation of the glycosidic linkages. Similarly, Arboleda and Loppnow found that their Raman spectra of each of nine different monosaccharides were unique (Arboleda and Loppnow 2000). These monosaccharides were *O*-methylated to block racemization of the anomeric carbon. The authors found that they could even distinguish between the α- and β-anomers of several of these monosaccharides. They also reported that such distinctions could be made on samples of less than 0.1 mg, though typically larger amounts are generally used in most studies. Arboleda and Loppnow were also able to use Raman marker bands to identify the monosaccharide components of unknown disaccharide samples (Fig. 3).

Although carbohydrates do not display as well-defined coordination properties as many other natural ligands, they do bind transition metal ions. The large number of electronegative functional groups and well-defined stereochemistries of sugars makes them attractive synthons for the synthesis of more complex structures. The mode of coordination of metal ions with the different hydroxyl groups of sugars is a subject of importance for guiding new syntheses, but quantitative characterization of the anomeric and conformational species of the carbohydrates involved in these complexes is difficult. Cerchiaro et al. used Raman spectroscopy and electron paramagnetic resonance (EPR) to investigate complexes of Cu(II) ions with D-glucose, D-fructose, and D-galactose (Cerchiaro et al. 2005). They found that

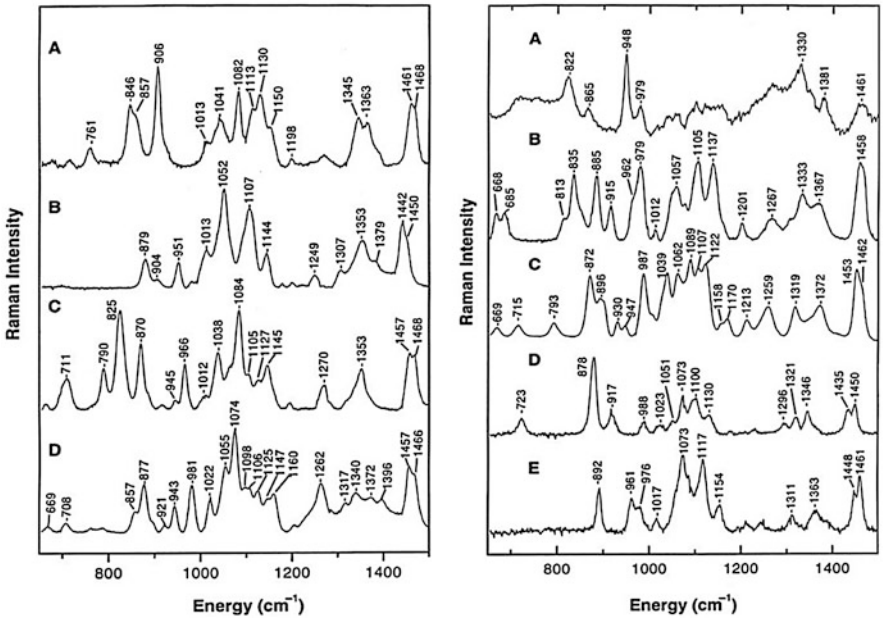

Fig. 3 Raman spectra of 1-*O*-methyl-monosaccharides. *Left-hand panel*: (*A*) 1-*O*-methyl-α-D-glucoside, (*B*) 1-*O*-methyl-β-D-glucoside, (*C*) 1-*O*-methyl-α-D-galactoside, and (*D*) 1-*O*-methyl-β-D-galactoside. *Right-hand panel*: (*A*) 1-*O*-methyl-α-D-*N*-acetylgalactosamine, (*B*) 1-*O*-methyl-α-D-mannoside, (*C*) 1-*O*-methyl-β-D-mannoside, (*D*) 1-*O*-methyl-α-D-xyloside, and (*E*) 1-*O*-methyl-β-D-xyloside. All spectra were measured with 2 W of 514.5 nm light. Note that the label of the ordinate axis used here, "energy," means the same as the more common "wave number" and "Raman shift" labels (Figure is Adapted from Arboleda and Loppnow 2000)

the β-anomer was the dominant form of D-glucose when complexed, but both α- and β-anomers were found in the complexes of D-galactose. For the complexes of D-fructose, both furanose and pyranose forms were detected, with furanose being the major one. Specific hydroxyls and oxygens were also identified as being coordination sites for the Cu(II) ions, from changes in their signature Raman bands upon complexation.

Mixtures of simple sugars are commonly found, and overlap of Raman bands from these sugars can yield complex spectra. However, standard analytical tools can successfully resolve the differences between the Raman spectral signatures and hence the identities and relative contributions of each. A nice illustration of this is a teaching experiment designed by Wang and colleagues (2009), who used principal component analysis and regression models (PCA/PCR) from the Raman spectra to quantify the relative compositions of three sugars (D-(−)-fructose, D-(+)-glucose, and D-(+)-galactose) in a solution mixture. It is particularly noteworthy that in this study undergraduate students were able to use this approach to obtain accurate results.

Previously, Mrozek et al. had used both Raman and SERS spectroscopies to differentiate between two sugars, maltotetraose, and stachyose (Mrozek et al. 2004). Their reported SERS spectra, following a procedure developed by

Mrozek and Weaver to measure SERS of several monosaccharides (Mrozek and Weaver 2002), were very similar to the corresponding Raman spectra, but apparently with enhancement factors of 2–3 orders of magnitude, so significantly reducing detection limits. These authors also considered the question of separating and quantifying the spectral signatures of each of the two sugars in a binary mixture and found this could be achieved accurately using PLS algorithms.

As previously stated, one advantage of SERS as an analytical technique is that it does not require an extrinsic label. However, in cases where even higher signal enhancements are sought, facilitating even down to attomolar detection, a widely used strategy is to chemically link a chromophoric reporter group, typically a dye compound, to either the analyte molecule or the metal surface. This further electronic resonance enhancement gives rise to the technique of surface-enhanced resonance Raman scattering or SERRS. Vangala et al. adopted this approach and coupled rhodamine tags to three different sugars: glucose, lactose, and glucuronic acid (Vangala et al. 2010). These tagged carbohydrates were shown to increase sensitivity for not only Raman detection but also for fluorescence and mass spectrometric analysis as well.

All sugars are chiral, making Raman optical activity (ROA) an obvious technique for investigating their solvated conformations. The Barron group in Glasgow undertook a number of studies on small sugars and found that detailed and informative spectra could be measured (Bell et al. 1994a, b, 1995; Macleod et al. 2006). Most significantly, Wen et al. (1993) verified that ROA can determine the absolute configuration about each chiral center of a carbohydrate and differentiate between α- and β-anomeric linkages; that large ROA spectral differences can be observed between epimers; that ROA spectra can also discriminate between homomorphic sugars, which have the same stereochemistry around each chiral carbon but different substituents, though these spectral differences are weaker than those found for epimers; and finally, that ROA can infer the relative conformations of CH_2OH groups, which are important for intramolecular hydrogen bonding and for stabilizing backbone conformations.

Further studies were conducted on cyclodextrins (Bell et al. 1997; Barron et al. 1990), and these established that ROA can provide detailed information about the conformational dynamics of oligosaccharides. The first ROA spectra of glycoproteins were, again, first reported by the Glasgow group (Bell et al. 1994c; Smyth et al. 2001; Zhu et al. 2005), who then subsequently demonstrated that ROA could simultaneously probe the structural complexity of both the protein and glycan components of a glycoprotein (Johannessen et al. 2011).

3 Conformational Studies on Polysaccharides and Glycoproteins

Raman and ROA spectroscopies have also been used to characterize the conformations and behavior of complex polysaccharides. One notable example of this is the study by Yaffe et al. on hyaluronan (HA), a nonsulfated glycosaminoglycan (GAG)

composed entirely of repeating disaccharides of glucuronic acid (GlcA) and *N*-acetyl-glucosamine (GlcNAc) linked by alternating β-1,3 and β-1,4 glycosidic bonds (Yaffe et al. 2010). Hyaluronan is found in all vertebrate tissues as a high molecular mass polysaccharide and performs a wide range of biological functions, leading to its widespread use in medicine, tissue engineering, and cosmetics. However, we understand relatively little about the structural parameters that regulate hyaluronan organization and function. Yaffe et al. were able to use the stereochemical sensitivity of ROA in order to monitor characteristic intersaccharide interactions in a short hyaluronan subunit (the HA_4 tetramer) but then found that there were no signs of extensive interchain interactions being formed in a much longer HA chain (see Fig. 4). In this way, the authors were able to conclude that there was no extensive tertiary structure formation in the HA polymer, in agreement with several NMR studies (Kaufmann et al. 1998; Blundell et al. 2006).

Rudd et al. have also reported the Raman and ROA spectra for several glycosaminoglycans (Rudd et al. 2010), further emphasizing the potential of the technique in glycobiology.

Recently, Ashton et al. have used both Raman and ROA spectroscopies to investigate the interactions between mucin glycoproteins (Ashton et al. 2013). Mucins are highly glycosylated, high molecular weight proteins which perform diverse roles in the formation of mucosal gels in metazoans. Mucins are important for determining the physical properties of gastrointestinal and salivary mucus, and they function as mesh-like, size, and charge exclusion barriers. Most mucins have a block copolymer structure with nonglycosylated domains at both termini that are separated by an extended glycosylated domain which is rich in serine, threonine, and proline residues. O-Linked glycosylation occurs through conjugation of *N*-acetylgalactosamine (GalNAc) sugars to the hydroxyl moieties of the serines and threonine side chains, giving rise to the so-called hinge region that is thought to be important for molecular control of the formation of the mucosal mesh. Using 2D correlation analysis with both Raman and ROA spectra, the authors were able to distinguish the order of conformational changes occurring over concentration ranges relevant to the formation of the gastric mucosal layer. They found that at mucin concentrations from 20 to 40 mg/ml, these GalNAc moieties underwent conformational changes, with other saccharides changing conformation above 40 mg/ml, together with other structural transitions observed in the protein core, specifically the formation of β-structure. In this way, Raman and ROA were able to monitor the formation of transient entanglements formed by what are thought to be brush–brush interactions between the oligosaccharide combs of mucin molecules.

One particular great challenge for glycobiology is to map and understand the expression patterns of component sugars in the glycan components of glycoproteins. With most techniques it is difficult to determine linkage types and between oligosaccharides with similar compositions. Johannessen et al. examined yeast invertase from *S. cerevisiae*, a high-mannose glycoprotein that is widely used in the sugar industry as a biocatalyst, and a number of its component oligosaccharides. Structures of these sugars are shown in Fig. 5 along with the Raman and ROA spectra of the mannose monosaccharide and three disaccharides. Unsurprisingly,

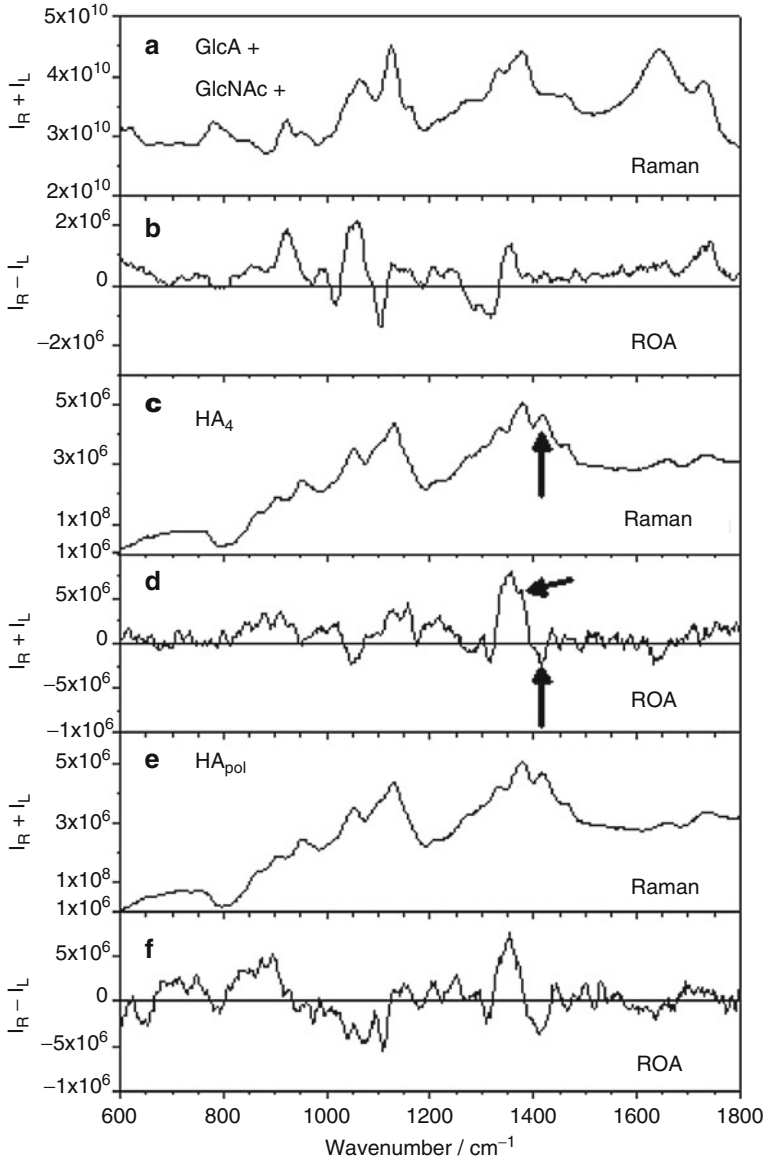

Fig. 4 Raman ($I_R + I_L$) and ROA ($I_R - I_L$) spectra, respectively, of a 1:1 stoichiometric mix of GlcA and GlcNAc (panels *A* and *B*), HA_4 tetramer (panels *C* and *D*), and the HA_{pol} polymer (panels *E* and *F*). Secondary structure marker bands are shown with *arrows*. The large differences between the ROA spectra shown in panels *B* and *D* reflect the formation of secondary structure-type interactions between saccharides, while the strong similarity between the ROA spectra for HA_4 and HA_{pol} (panels *D* and *F*) indicates that no significant tertiary interactions are formed in the polymer (Figure is taken from Yaffe et al. 2010)

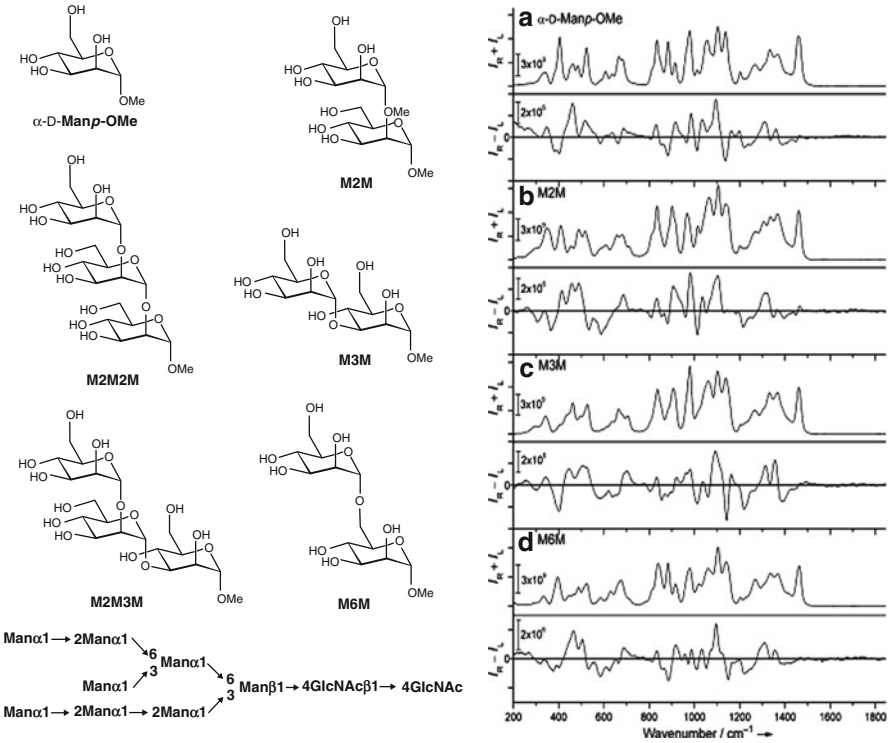

Fig. 5 Shown on the *left* are the structures of mannose oligosaccharides found in yeast invertase, along with the linkage scheme of the $Man_8GlcNAc_2$ unit. On the *right* are the corresponding Raman and ROA spectra for the mannose mono- and disaccharides (Figure is taken and adapted from Johannessen et al. (2011))

the four Raman spectra are all similar, though with some differences in detail. Far more significant differences can be observed between their corresponding ROA spectra. The obvious changes in ROA band profiles and intensities originate from the different glycosidic linkages and the resulting effects on conformation and dynamics of the component sugars.

Further differences between the ROA spectra were observed for the two mannose trisaccharides, labeled as M2M2M and M2M3M, and measured by Johannessen et al., as is shown in Fig. 6. Most strikingly, the complex ROA band structures from ~250 to 700 cm^{-1}, shown by shading, present in the spectra of M2M2M and M2M3M are also clearly apparent in the ROA spectrum of the yeast invertase. The authors concluded that this band pattern originated from the α-(1 → 2)- and α-(1 → 3)-glycosidic linkages, possibly with some minor contributions from α-(1 → 6)-linkages. As the authors stated, this close similarity in ROA band patterns also indicated that the conformations around these glycosidic links in the glycoprotein are very similar to those of the free mannose trisaccharides in aqueous solution. Although the use of Raman spectroscopies for studying protein

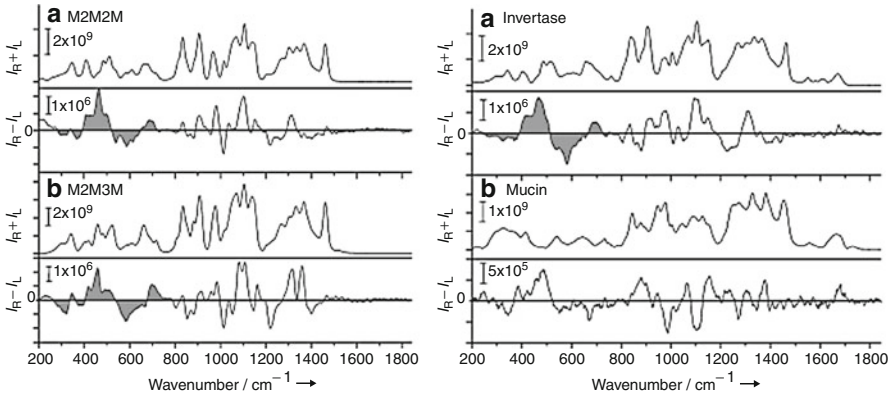

Fig. 6 Shown on the *left* are the Raman and ROA spectra for the mannose trisaccharides α-D-Man*p*-(1 → 2)-α-D-Man*p*-(1 → 2)-α-D-Man*p*-OMe (M2M2M) and α-D-Man*p*-(1 → 2)-α-D-Man*p*-(1 → 3)-α-D-Man*p*-OMe (M2M3M). Presented on the *right* are the Raman and ROA spectra of (*a*) yeast external invertase and (*b*) bovine submaxillary mucin in water. The shaded ROA band pattern in the low-wave number region of the invertase spectrum is very similar to the shaded patterns in the ROA spectra of the trisaccharides M2M2M and M2M3M (Figure is taken and adapted from Johannessen et al. 2011)

structure lies outside the purposes of this review, it should be noted that Raman spectroscopies, including ROA, can simultaneously probe both the protein and carbohydrate moieties of a glycoprotein. Johannessen et al. were able to determine from the absence of protein structural ROA marker bands that invertase was completely disordered, presumably due to the glycan content, similarly to a commercial sample of the highly glycosylated bovine submaxillary mucin.

Recently, this group extended their study on glycoproteins to ribonuclease B (RNase B). As already described, RNase B has the same protein sequence as RNase A as well as a single N-linked glycan with two GlcNAcs and a variable number of mannose residues. These researchers were able to reconstruct the Raman and ROA spectral signatures for this glycan component, as shown in Fig. 7, by subtracting the protein spectral signatures measured for the nonglycosylated RNase A (Mensch et al. 2014). Although there is insufficient information yet to analyze the glycan spectra in detail, this work demonstrates the future potential for Raman spectroscopies for investigating the structures of the glycan moieties of glycoproteins in situ.

4 Probing Hydration Interactions of Sugars

The dynamics of water molecules have long been thought to play important roles in the behavior and properties of carbohydrates. Water is a weak Raman scatterer so making Raman measurements on aqueous solutions easier than when using infrared spectroscopy. However, Raman spectra of solutes, including carbohydrates, are

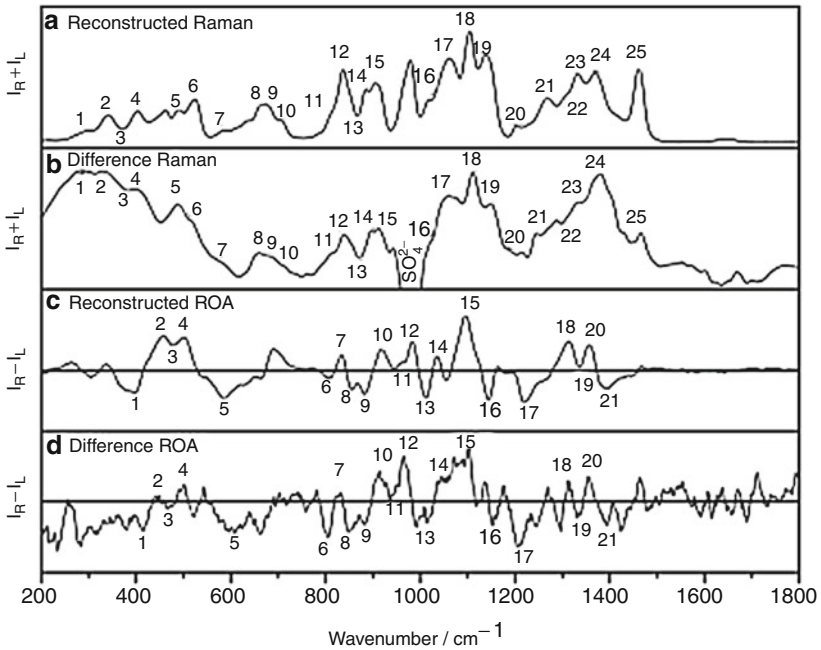

Fig. 7 Reconstructed Raman (*A*) and ROA (*C*) spectra of the glycan moiety from RNase B from the constituent disaccharide spectra and difference Raman (*B*) and ROA (*D*) spectra of RNase B after subtraction of the respective RNase A spectra. Particular bands are numbered (Figure is taken from Mensch et al. 2014)

sensitive to interactions with water molecules. Soderholm et al. investigated the sensitivity of specific Raman bands to hydration for samples of glucose and fructose (Soderholm et al. 1999). In their study of honey samples, de Oliveira et al. found that Raman bands of the component saccharides showed subtle changes in relative intensity as a function of water content (de Oliveira et al. 2002). Paola Sassi and colleagues in Perugia have performed a number of studies on hydration interactions with carbohydrates using different biophysical techniques including Raman spectroscopy (Fioretto et al. 2007; Paolantoni et al. 2007). They have shown that Raman bands from solvent water molecules are sensitive to the disordering of tetrahedral water structures by sugar molecules (Gallina et al. 2006; Perticaroli et al. 2008), with glucose and fructose appearing to have a different effect on bulk water structure than trehalose and dextran.

Irradiation of foods is now a widely used method for controlling microbial and insect contamination and can also extend the shelf life of fruits and vegetables by delaying ripening and inhibiting sprouting. However, ionizing radiation can, of course, cause chemical damage, and in the case of carbohydrates, this can lead to both the direct breaking of chemical bonds and indirect effects from formation of reactive hydroxyl radicals from water molecules within the foodstuffs.

5 Characterizing the Chemical Modification of Sugars

Raman spectroscopies show particular promise for the identification of chemical modifications in carbohydrates, particularly of sulfation. The vibrational modes of the sulfonyl group are typically intense and sharp and so are often easy to distinguish from the many other vibrational modes of carbohydrates, as was shown many years ago (Bansil et al. 1978; Cabassi et al. 1978). More recently, a number of other research groups have further explored the capabilities of Raman techniques for studying the sulfation of glycosaminoglycans. Matsuhiro and colleagues (2012) combined Raman and SERS spectroscopies in addition to FTIR and NMR to investigate the composition of material extracted from a sea cucumber (*Athyonidium chilensis*). They found that the SERS spectra were more informative than the corresponding Raman spectra, and their collective experiments characterized the glycosaminoglycan composition of the extract, with chondroitin 4,6-disulfate substituted at position O-3 of glucuronic acid and partially 2,4-disulfated-fucopyranosyl residues being found.

6 Industrial and Healthcare Applications

One of the greatest challenges currently facing the pharmaceutical sector is the characterization of posttranslational modifications (PTMs) of protein pharmaceuticals, with the most common of these being glycosylation. The stability, immunogenicity, and pharmacokinetics of a protein drug can all be affected by glycosylation, but detection and characterization of the glycan content typically require complex, destructive, or time-consuming methodologies. Raman spectroscopy has the potential to meet the requirement for a fast, noninvasive, and quantitative technique for the characterization of the glycan content of protein pharmaceuticals. Brewster et al. demonstrated that Raman spectroscopy coupled with multivariate data analyses could differentiate between the nonglycosylated ribonuclease A (RNase A) and the glycosylated ribonuclease B (RNase B, which has an identical amino acid sequence but also a single N-linked glycan containing two GlcNAcs and from three to nine mannoses), as well as deglycosylated versions of RNase B (Brewster et al. 2011). The Raman spectra shown in Fig. 8 display significant differences, highlighted in purple, due to glycosylation. Using the first principal component from the resulting PCA analysis performed on these Raman spectra, the authors were able to clearly distinguish between the glycosylated (RNase B) and nonglycosylated (RNase A) proteins.

Raman bands are quantitative, and the authors were also able to use another chemometrics technique, principal least squares regression (PLSR), to show that this methodology could accurately determine the amount of carbohydrate in a glycoprotein. In their results, presented in Fig. 9a, we observe the strong correlation between the predicted and known proportions of RNase B in mixtures of RNase A and B. Although this was a proof-of-principle experiment on a simplified system, this work is a good exemplar of the use of Raman for quantitative glycobiology.

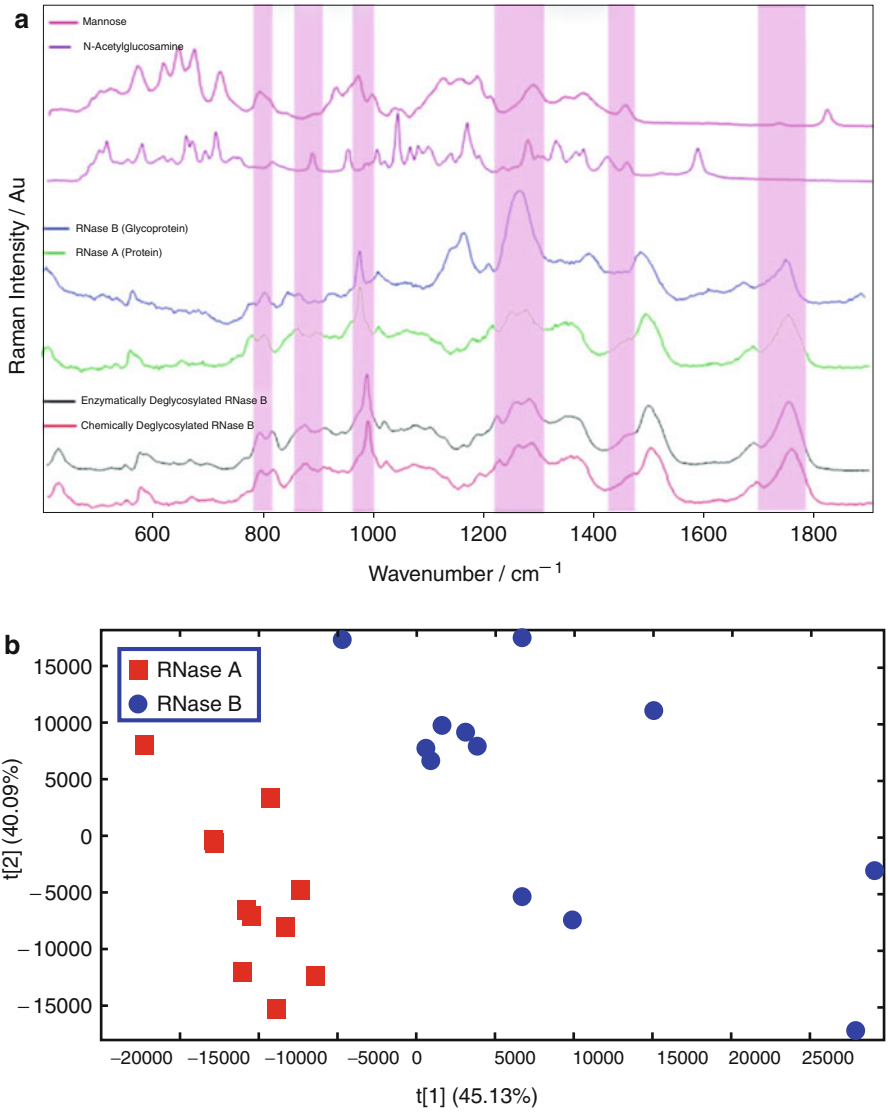

Fig. 8 Panel (**a**) shows averaged Raman spectra of mannose, GlcNAc, ribonuclease A and B, and chemically and enzymatically deglycosylated ribonuclease B, measured at 785 nm. Areas highlighted are regions of significance, as indicated by the PLS loading in panel (**b**), which presents the PCA scores plot (PC1 vs. PC2) of the ribonuclease data, showing ribonuclease A and B spectra resolved into separate clusters allowing separation of the glycosylated and nonglycosylated forms (Figure is taken from Brewster et al. 2011)

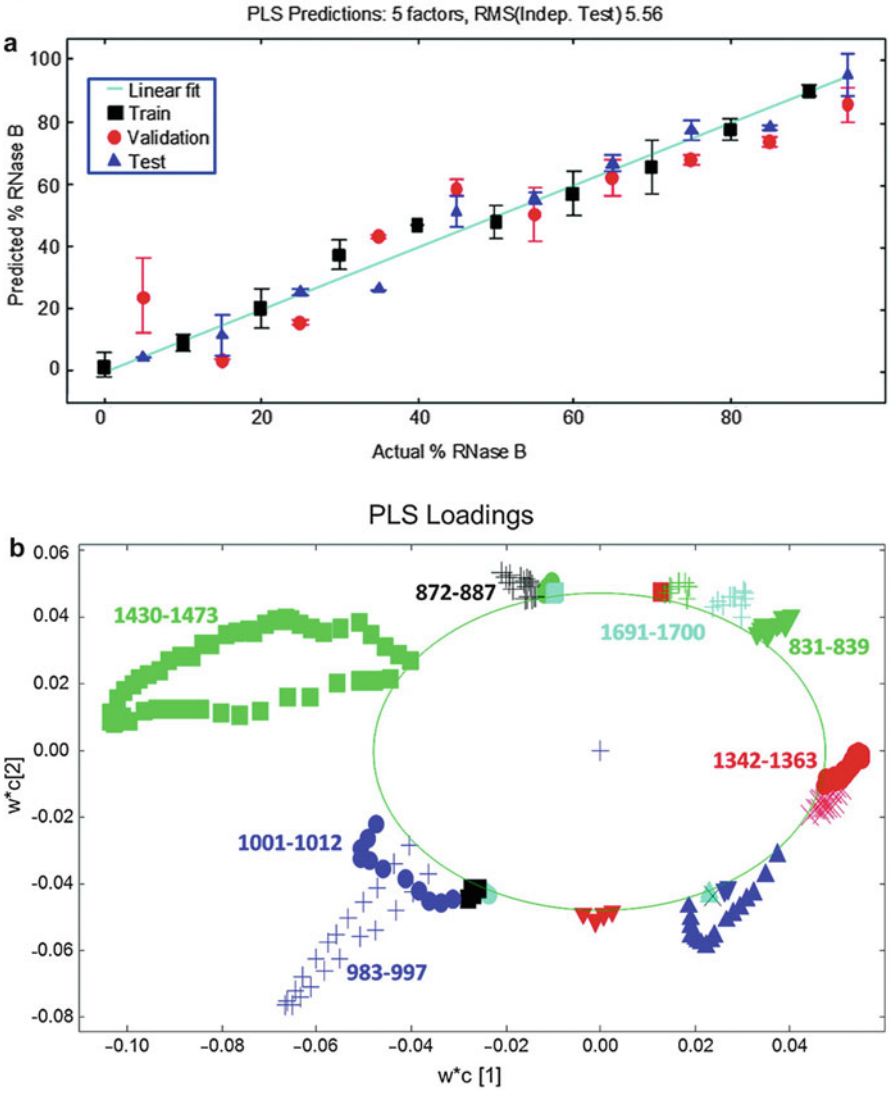

Fig. 9 (**a**) PLS predictions from Raman data of RNase mixtures (mean predictions (from $n = 5$) are plotted with standard error bars). (**b**) PLS loading plot of the first two latent variables (LVs; w_c[1] vs. w_c[2]); the *green circle* indicates the 95 % confidence limit. *Numbers* shown refer to Raman peak positions (Figure is taken from Brewster et al. 2011)

Furthermore, chemometrics analyses can also reveal greater structural detail from complex Raman spectra. Panel (b) of Fig. 9 shows the PLS loading plot from this study, with the first two latent vectors, which were responsible for most of the variance in this data, being sensitive to relative changes in selected marker bands from the regions highlighted in Fig. 8a.

A long-standing bioanalytical challenge is the detection and control of glucose levels in the bloodstream, for the control of diabetes mellitus. Among many other techniques, Raman spectroscopies have been applied to this problem. In particular, the van Duyne group at Northwestern University has developed nanolithographic surfaces as SERS-based sensors for monitoring glucose levels (Schafer-Peltier et al. 2003; Lyandres et al. 2005). More recently, this group has used a specialized spatially offset form of SERS for transcutaneous monitoring of glucose within living rats (Yuen et al. 2010; Ma et al. 2011). An alternative approach to monitoring glucose levels directly has been explored by Barman et al. who propose the detection of glycated hemoglobin (HbA1c), which is known to display a strong correlation with bloodstream glucose levels and is an approved target for screening diabetic and prediabetic conditions (Barman et al. 2012). These researchers coupled Raman excitation at 785 nm with drop coating deposition (DCD), which is a relatively new but popular analytical Raman technique (Ortiz et al. 2006). In brief, DCD uses special hydrophobic surfaces to preconcentrate the analytes in dried solution samples, so greatly increasing signal intensity. Analytes tend to coalesce into a coffee-ring pattern, and this phenomenon is still a subject of investigation, particularly with reference to the homogeneity of material deposited within the ring. Through their experiments on both HbA1c and nonglycated hemoglobin (Hb), Barman et al. found that DCD Raman combined with PCA and PLS informatics could distinguish spectra signatures of HbA1c that provided a limit of detection (LOD) of as low as 3.8 μM. This compares very favorably with clinically determined concentrations of HbA1c (60 μM and higher). Figure 10 shows how the PCA scores plot generated from their DCD Raman data could directly differentiate between the glycated HbA1c and nonglycated Hb. Although this paper by Barman et al. was another proof-of-principle experiment, they also consider in some detail the potential of this approach for clinical application, and we direct interested readers to their paper as well as a similar study on glycated albumin (Dingari et al. 2012).

The long-term and widespread prevalence of carbohydrates in foods and beverages makes the food and drink industry an obvious sector of interest for Raman spectroscopies. The rapid, noninvasive, and label-free nature of Raman scattering makes it well suited to many situations in food science and agriculture, though the complexity of spectra from food samples often requires the use of informatics during data analysis. Such a strategy was followed by Delfino et al. in their use of a standard Raman microscope to quantify glucose content in different commercial sports drinks (Delfino et al. 2011). They collected Raman spectra with a simple He–Ne laser and 50× optical objective on droplets of sample, with example spectra being shown in Fig. 11. Interval partial least squares (iPLS) was then employed to identify key marker bands and construct calibration models that allowed accurate determination of glucose concentration, within experimental error of the results from enzymatic assays.

Although the result from each Raman analysis had a higher experimental uncertainty than for the corresponding enzymatic (biochemical) assay, as is apparent in Fig. 12, this work shows that accurate quantitative analysis of sugars can be

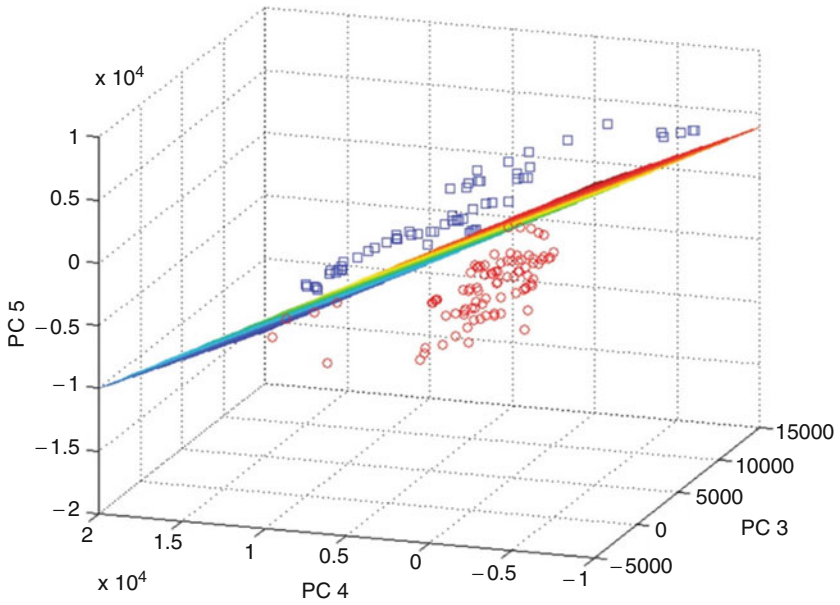

Fig. 10 Three-dimensional scores plot corresponding to principal components (*PCs*) 3, 4, and 5 for the Raman dataset acquired from single-protein Hb and HbA1c drop-coated rings. Hb samples are indicated by *red circles* and HbA1c by *blue squares* (Figure is taken from Barman et al. 2012)

obtained using relatively standard Raman equipment and multivariate analytical tools and a simple calibration model. As such Raman analyses of carbohydrates in food and beverage samples could be made rapidly and without specialist sample preparation, there is great potential for such techniques in on-site quality control and characterization of foodstuffs and beverages.

7 Applications in Virology

Glycoproteins play critical roles in the mechanisms of viral infection, such as membrane fusion, with conformational changes in these glycoproteins being important for driving these mechanisms. As already mentioned, conventional structural techniques are often difficult to apply to this problem. In the requirement for rapid clinical diagnosis of viral infection, the time constraint becomes increasingly important. The fast data acquisitions inherent to Raman technologies, coupled with the wealth of structural information that can be obtained, are leading to their application in structural virology, including the roles of glycoproteins in viral infection and cell–cell fusion. Lu et al. (2013) have used a confocal Raman microscope, along with chemometrics, to discriminate glycoproteins on the surfaces of virions and viruslike particles (VLPs) of Nipah virus (NiV). NiV is an

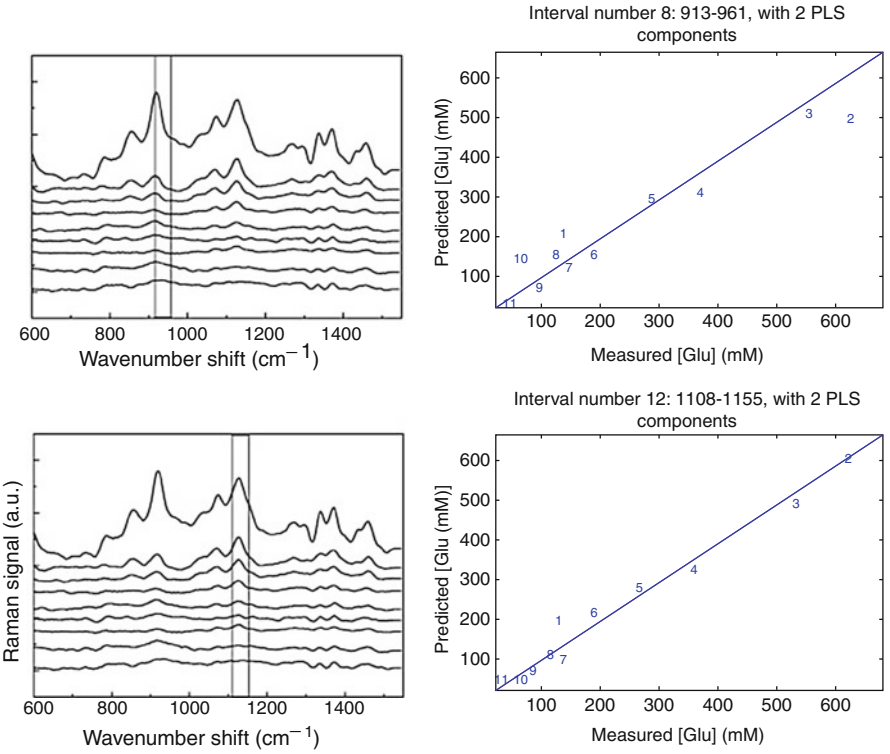

Fig. 11 Selected spectra intervals used in the iPLS model (*left panels*) for Raman spectra of solutions of different glucose concentrations with the corresponding predictions of concentration obtained using single spectral intervals (*right panels*, from 913–961 cm^{-1} (*top*) to 1,108–1,155 cm^{-1} (*bottom*)). Characteristic Raman marker bands for the α- and β-anomers are found at 919 and 1,128 cm^{-1}, respectively. *Numbers* represent the identities of individual measured spectra (Figure is taken from Delfino et al. 2011)

enveloped virus from the *Paramyxoviridae* family and zoonosis that is a disease that crosses species barriers and that causes severe illness in humans (encephalitis and respiratory disease) with a 40–75 % mortality rate and no approved therapy. Its relative aerosol stability and propensity for cross-species infection make NiV a potential bioterrorism agent and a priority pathogen for the National Institutes of Health and other healthcare authorities. In NiV, the F- and G-glycoproteins are required for membrane fusion during cell entry and pathognomonic cell–cell fusion. Figure 13 shows Raman spectra collected by Lu et al. for various NiV VLPs and pseudovirions expressing the F- and G-glycoproteins, as well as the matrix (M) protein.

A commonly used method for differentiating between similar Raman spectra such as those shown in Fig. 14 is to take the second derivative, with these derivatives being shown for NiV-M, NiV-G, and NiV-F in Fig. 14, panels (a) and (b). Second-derivative Raman spectra are very sensitive to differences in identity and

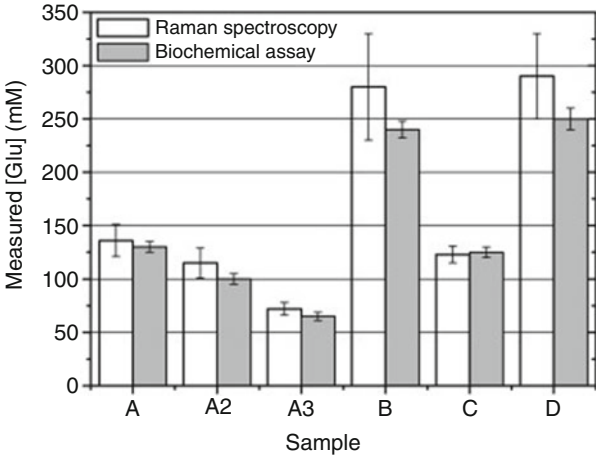

Fig. 12 Measured glucose concentrations for the investigated commercial beverage samples as obtained by iPLS analysis of Raman spectra, benchmarked against the enzymatic (biochemical) assays (Figure is taken from Delfino et al. 2011)

composition, and Lu et al. were able to utilize these for constructing a PCA model, shown in panel (c) of Fig. 14, which could clearly differentiate between the three VLPs based on the glycoproteins expressed. The rapid capability of Raman spectra to characterize viruses and identify structural changes makes it a viable real-time diagnostic technique for virology and vaccine development.

Raman spectra are sensitive to the specific vibrational modes that characterize changes in the structure of biomolecules, so making it an increasingly important biophysical technique. An example of this is presented here from the Lu et al. paper in Fig. 15, where they used the second derivatives of the measured Raman spectra in order to increase spectral sensitivity and remove the effects of baseline variations. Panels (a–c) display characteristic spectral changes induced by receptor binding to the F- and G-glycoproteins attached to the NiV pseudovirions. The authors suggested that they were probably monitoring the formation of a prehairpin intermediate. Note that no conformational change occurs in panel (d), and the two traces overlap perfectly. This work illustrates both the applicability of Raman spectroscopies to studying large biomolecular complexes, such as virions, and the sensitivity of specific marker bands to conformational changes, in this case in glycoproteins.

8 Studies on Carbohydrates Within Living Cells

Raman spectra can also be readily obtained from living single cells, such as bacteria and yeast, using microscope systems. Standard methods used for monitoring the uptake and metabolic flux of nutrients, such as sugars, typically involve isotopic labeling combined with biophysical methods such as chromatography or mass spectrometry. These approaches are complex and time-consuming and require bulk cell populations and experiments performed on cell extracts, so potentially losing information about the effects of cellular variation and dynamics.

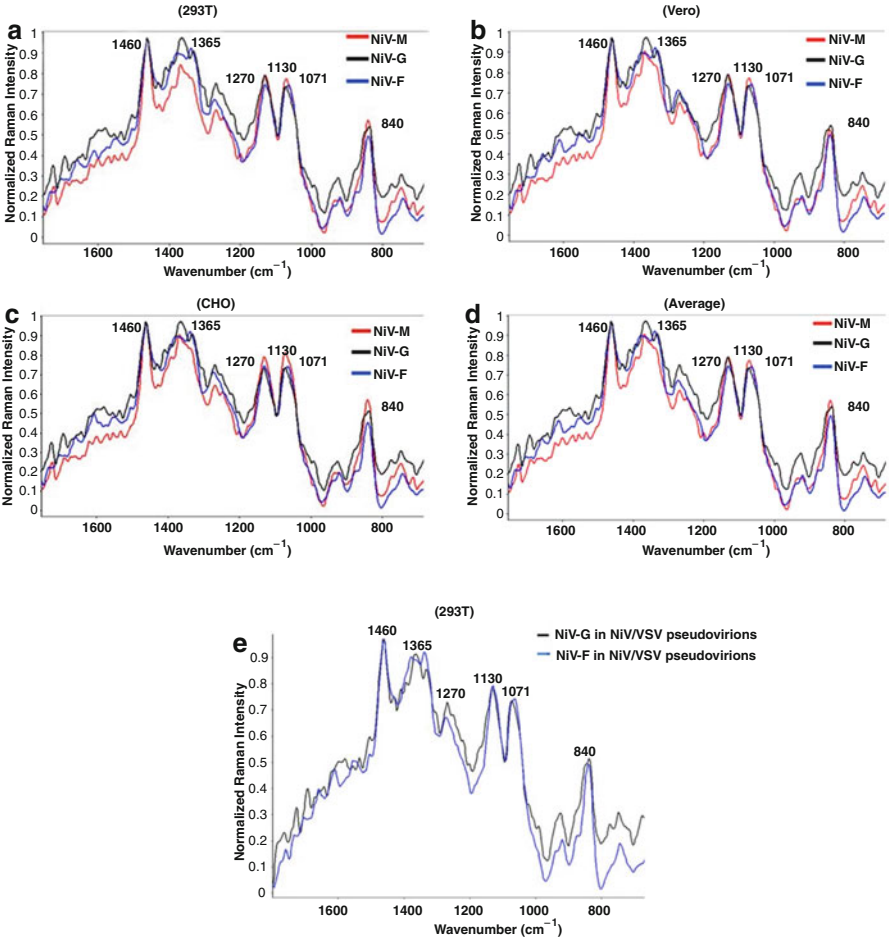

Fig. 13 Raman spectral features of M-, F-, and G-proteins on NiV VLPs cultivated in three different cell lines (panels **a**–**c**), the average of VLP signals produced from three distinct cell cultures (panel **d**), and NiV-G and NiV-F spectra from pseudovirions (panel **e**) (Figure is taken from Lu et al. 2013)

While fluorescent labels and stains can reveal useful information about sugar uptake and metabolism, this approach introduces potential problems due to the size and chemistry of exogenous fluorophores affecting the structure and behavior of the investigated biomolecules, issues of inhomogeneous expression and distribution, as well as photobleaching reducing signal intensity and reproducibility. The ability of Raman microscopy to measure detailed chemical and structural information from intrinsic vibrational motions of carbohydrates, without the requirement of a fluorescent label being added, makes it a more widely applicable and label-free probe of carbohydrate biochemistry in living cells. A recent demonstration of this can be found from the work of Avetisyan et al. (2013). This group used laser

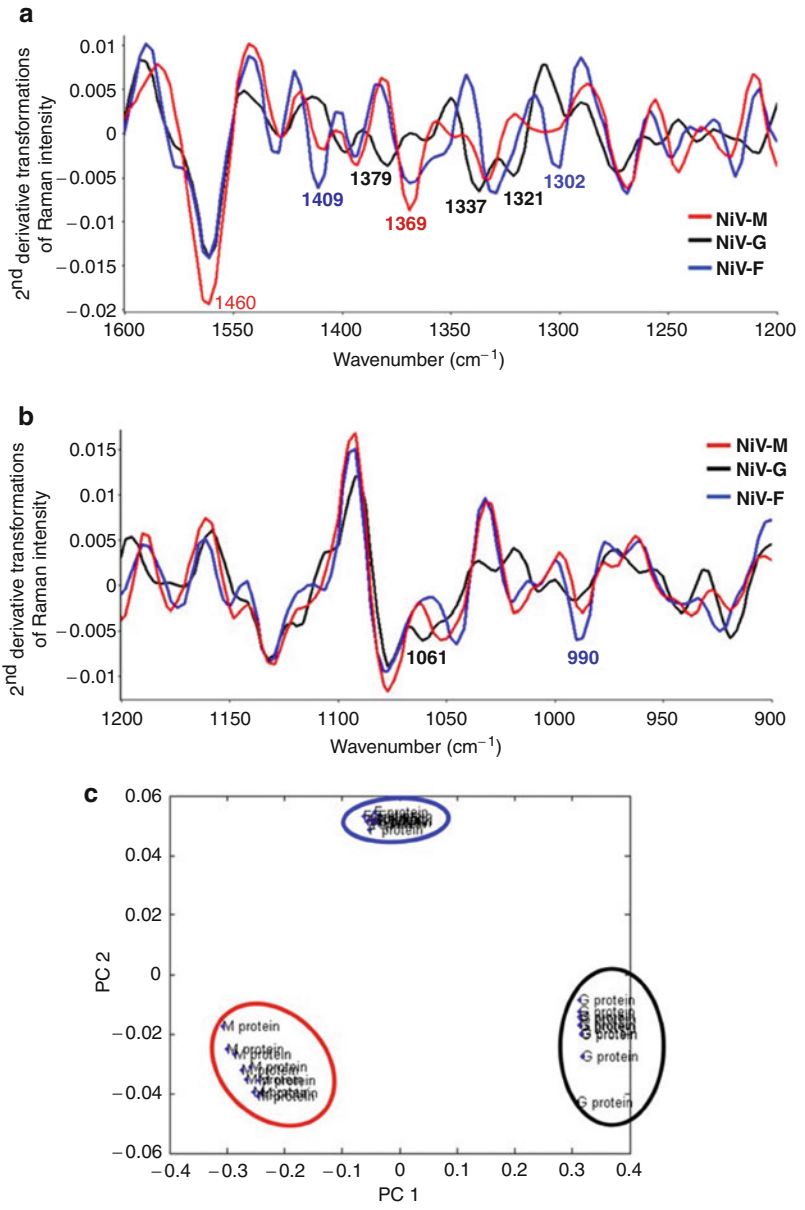

Fig. 14 Second-derivative analyses of Raman spectral features showing specific M, F, and G spectral peaks. Panel (**a**) shows the second-derivative transformation of Raman spectra (1,500–1,200 cm^{-1}) of the M-, F-, and G-proteins on NiV VLPs (from the *Vero cell line*). Panel (**b**) shows the same as for panel (**a**) but for the range of 1,200–900 cm^{-1}. Panel (**c**) shows a representative PCA classification model established and cross-validated to differentiate NiV proteins (*n*_4), with data points being circled as *blue*, F-protein; *black*, G-protein; *red*, M-protein (Figure is taken from Lu et al. 2013)

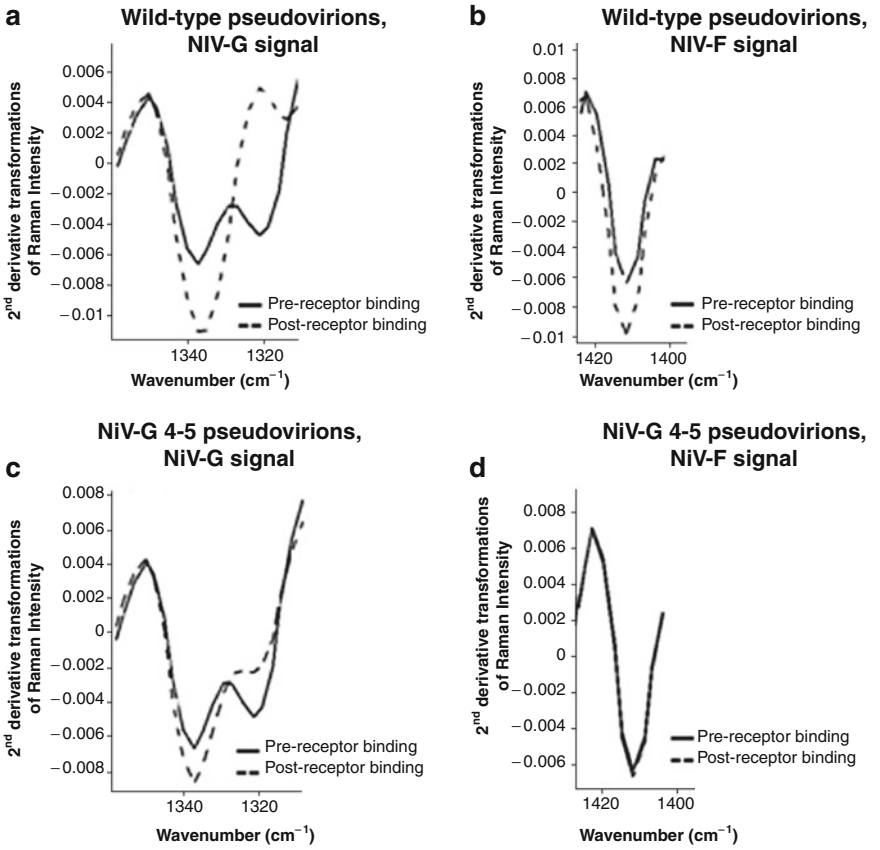

Fig. 15 Examples of Raman spectral changes (from the second derivative) corresponding to receptor-induced conformational changes in the NiV-F and NiV-G-glycoproteins. In panels (**a**–**c**) conformational changes are monitored but not in panel (**d**) (For specific details of these experiments please refer to Lu et al. 2013)

tweezers to isolate and localize single *Sinorhizobium meliloti* cells, a soil bacterium, and then collected Raman spectra at 785 nm to investigate the uptake of trehalose. This approach is also referred to as laser tweezers Raman spectroscopy (LTRS).

Figure 16 shows the sensitivity of Raman spectra to a small chemical difference in the disaccharide trehalose, in this case substitution of a single hydroxyl with a carbonyl moiety. Through following such changes in characteristic marker bands, Avetisyan et al. could monitor uptake and metabolism of trehalose by individual *S. meliloti* cells, as is shown in Fig. 17. Although care must be taken to minimize the risk of photodegradation, the use of longer-wavelength lasers (in this case 785 nm) and short spectral acquisition times (as low as 10 s in this study) can achieve this. The authors were able to quantitatively follow the metabolism of trehalose in situ, determining that intracellular concentrations of the disaccharide were an average of

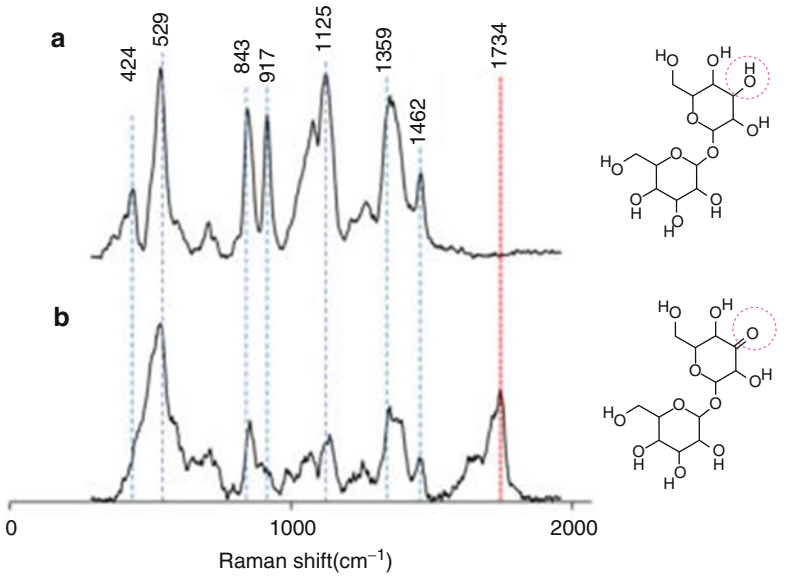

Fig. 16 Chemical structures (*right*) and Raman spectra (*left*) of a 5 % (w/v) aqueous solution of trehalose (*A*) and 3-ketotrehalose (*B*). Significant spectral differences are observed between the two closely related sugars, such as the carbonyl stretching vibration at 1,734 cm^{-1} distinguishing 3-ketotrehalose from trehalose. Key Raman peaks are labeled (Figure is taken from Avetisyan et al. 2013)

22 mM but varied from 18 to 65 mM. As the authors point out, their approach could be readily adapted for studies on carbohydrate metabolism, utilization, or production in a wide range of microorganisms.

Raman imaging is now a widely used technique in biomedical and materials research as it allows the direct visualization of the chemical complexity of surfaces and living material. To date, there have been few developments in the imaging of carbohydrates, but one relevant paper is that of Åkeson et al. who used coherent anti-Stokes Raman (CARS) spectroscopy to image both glucose fluxes in lipid bilayer vesicles and the metabolic responses to a glucose pulse by living yeast cells (Åkeson et al. 2010). Examples of their results on yeast cells are shown in Fig. 18, with a specific Raman vibration at 2,870 cm^{-1} being used to generate the images. For readers new to Raman spectroscopic imaging, please refer to more extensive reviews of this topic, e.g., Dochow et al. (2011), Chan (2013), Diem et al. (2013), Galler et al. (2014), Xu et al. (2014), but the key conceptual difference to fluorescence imaging is that in the various Raman imaging techniques images of a picture or map can be generated using any of the spectral marker bands measured. In this way, the chemistry of the sample, or changes in its chemical profile, is directly observed and spatially resolved, providing a powerful means to investigate the biochemistry of living cells and tissues in situ and in real time. In this case, Åkeson et al. were able to probe metabolic changes throughout all regions of a living cell induced by the glucose pulse.

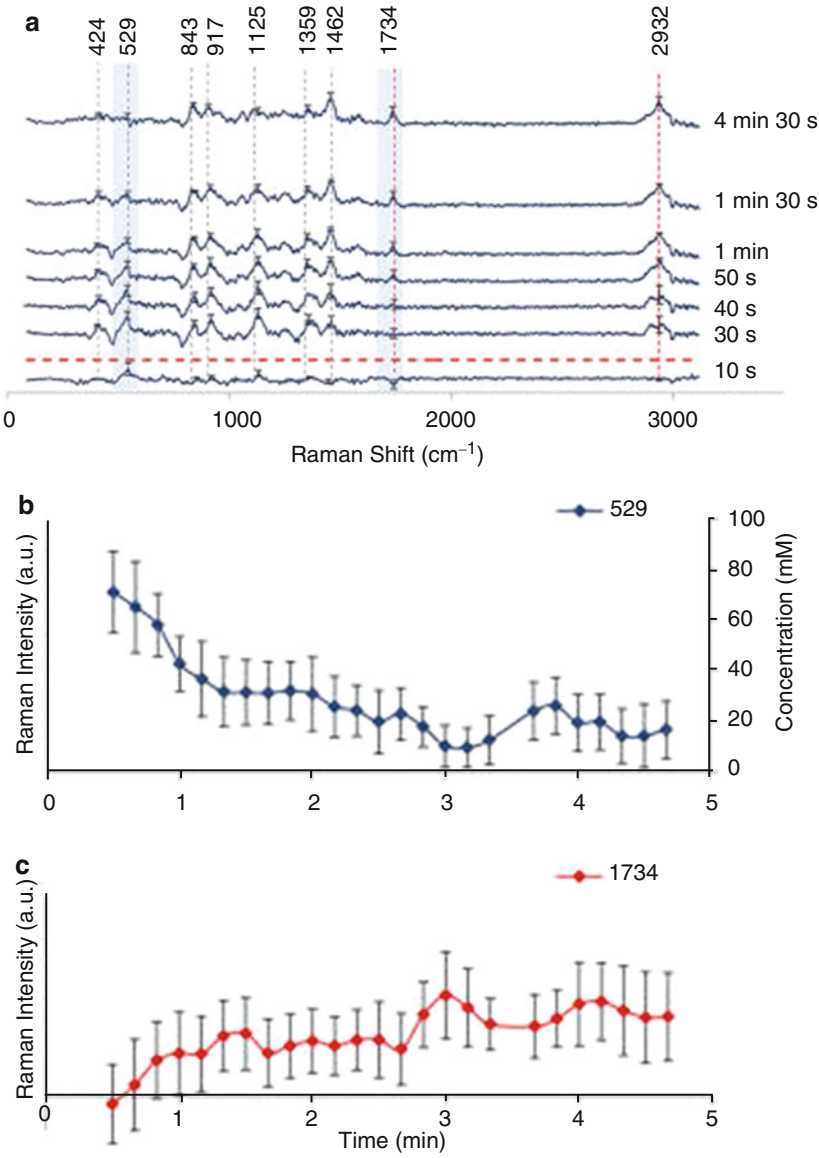

Fig. 17 (**a**) Time dependence of trehalose uptake and metabolism in single *S. meliloti* cells. Spectral average with standard error represents three different cells. Note that the acquisition time for each spectrum was 10 s (excitation power of 30 mW at 785 nm). Data are presented as continuous acquisitions of a single cell for 4 min and 30 s where the initial cell spectrum, i.e., at $t = 0$ s, was subtracted. *Dashed gray* and *red lines* show the peaks present and absent in the trehalose standard, respectively. Decrease of the peak at 529 cm^{-1} and appearance of the band at 1,734 cm^{-1} are due to conversion of trehalose to 3-ketotrehalose. The intensity changes of peaks occurring from 30 s to 4 min and 30 s with standard errors ($n = 3$) are presented in (**b**), for peak at 529 cm^{-1}, and (**c**) for peak at 1,734 cm^{-1}) (Figure is taken from Avetisyan et al. 2013)

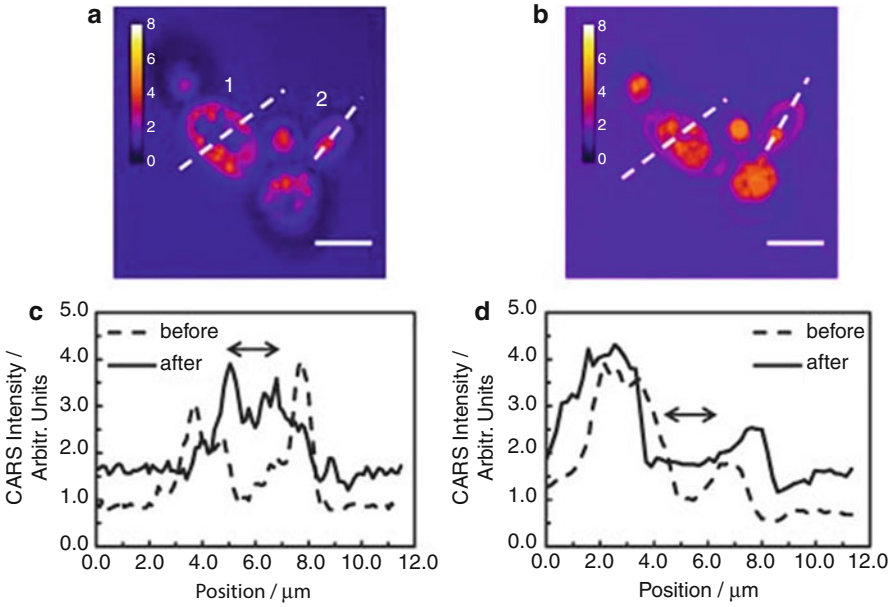

Fig. 18 CARS images (from the band at 2,870 cm^{-1}) of yeast cells before (**a**) and after (**b**) glucose addition. For the cells labeled *1* and *2*, the accompanying intensity profiles corresponding to the *dashed white lines* are shown in (**c**) and (**d**), respectively. After addition of glucose, increased CARS signals are observed both in the surrounding medium and within the cells. In addition, reduced cell size and a redistribution of organelles can be observed. The *horizontal arrows* above the graphs highlight the cytosol regions in the cells, characterized by higher CARS signal after addition of glucose compared to before. Image size is 25 × 25 µm (scale bar 5 µm), integration time 20 s (Figure is taken from Åkeson et al. 2010)

9 Computational Raman and ROA Spectroscopies

As shown above, experimental Raman and ROA spectroscopies can offer a great insight into the structure of carbohydrates. While a large amount of important data can already be elucidated in these cases, an even greater understanding can be exposed from using quantum chemical simulations.

This area of spectroscopy is one where there is a useful complement between the experimentally obtained data and computationally simulated spectra. It is possible to determine structural features, assign absolute configurations, or obtain otherwise unavailable vibrational data and structural dynamics. While early ab initio calculations of Raman intensities date back to the 1970s (Janosche 1973), the first reported ROA calculations came as late as 1989 (Bose et al. 1989), and following several important advancements in theory (Liegeois et al. 2007; Ruud and Thorvaldsen 2009) and computing, it is now possible to routinely simulate spectra of small- to medium-sized molecules.

ROA spectroscopy is a very powerful chiroptical technique and due to its treatment of chiral molecules makes it particularly useful for analyzing carbohydrates. Although while the combination of calculated and experimental data makes this method ideally suited to study these molecules, especially in light of shortcomings of other structural biology techniques, there are very few publications in this area. This is in part due to the difficulty of carrying out accurate calculations. Carbohydrates exhibit strong solvent effects requiring accurate treatment of water as well as exhibiting high conformational flexibility, meaning multiple calculations are needed to simulate the conformational dynamics. With these complications, the calculations can be computationally expensive, with full quantum simulations usually difficult on molecules larger than a few monosaccharides.

The computational treatment of carbohydrates using ROA spectroscopy is still very much an up-and-coming field, and as such much of the work referenced within this section focuses on understanding the structure of monosaccharides, and no work has been reported on larger molecules. As such the higher-order structure of carbohydrates has yet to be explored in this way. However, with refinements to the techniques, it is possible to get very accurate representations of experimental spectra with future aims to increase the size and scope of the research being carried out in this area.

9.1 Calculation of Raman and ROA Spectra

When carrying out the calculation of Raman and ROA intensities, it is important to use a suitable method and basis set. The early reported calculations utilized Hartree–Fock or multi-configurational self-consistent field methods with relatively small basis sets, and due to computational constraints at the time, only very small molecules could be studied (Polavarapu 1990; Barron et al. 1991a, 1992; Helgaker et al. 1994). Advancements in the theory as well as computation mean that DFT methods are now considered the standard in this area, and as such several benchmark studies have been carried out to find the most suitable functional and basis sets.

Early benchmark studies examined the importance of the basis set used for calculation of ROA. Pecul and Rizzo found that diffuse functions are an essential part of the basis set (Pecul and Rizzo 2003), and a more rigorous investigation by Zuber and Hug yielded a highly rarefied basis set called rDPS, constructed from 3-21++G with semi-diffuse p functions on all hydrogens that offered excellent results for ROA intensities when compared to much larger basis sets (Zuber and Hug 2004). In the basis set studies, Reiher et al. (2005) also examined the DFT method needed, finding that generalized gradient approximation and hybrid methods perform to a similar level, and both outperform local density approximation methods. In general several DFT functionals show potential but one of the most suitable choices is that of B3LYP, which exhibits a reasonable compromise between accuracy and cost (Ruud et al. 2002).

The most recent benchmark study published by Cheeseman and Frisch examined not only the basis set requirements for calculation of ROA and Raman intensities but also the requirements for optimization and calculation of the force field (Cheeseman and Frisch 2011). There are two different algorithms that can be used for simulation of the spectra: the one-step algorithm, where the force field and ROA invariants are calculated at the same level of theory, and the two-step algorithm, where the force field and ROA invariants are calculated at different level of theories. The authors offer suggested schemes for calculations of differing size systems; for small systems, the one-step procedure can be used, and the basis sets aug-cc-pVDZ and aug(sp)-cc-pVDZ are ideal. The two-step procedure however is more efficient and as such offers the ability to carry out calculations on larger systems. The recommend basis sets for medium to large systems are a combination of cc-pVTZ or 6-31G* with aug(sp)-cc-pVDZ or rDPS for the calculation of the force field and ROA tensors, respectively.

As mentioned above, the calculation of ROA spectra can be very time-consuming and computationally expensive, and as such calculations are limited to small- to medium-sized systems, meaning it can be difficult to get information about higher orders of structure of carbohydrates. To be able to expand calculations to larger systems, further approximations need to be made, and several have been suggested (Luber and Reiher 2009a; Ghysels et al. 2007) with one of the most popular being the Cartesian coordinate tensor transfer (CCT), proposed by Bour et al. (1997). This approach aims to calculate property tensors for large molecules by using values of overlapping smaller fragments. While some errors have been reported for this approach (Yamamoto and Bour 2011), it offers the scope of getting a greater structural understanding of larger carbohydrate molecules.

Due to the strong solvent effects that carbohydrates undergo, it is important to include an aqueous environment within calculations. There are three approaches that can be used to fulfill this: implicit solvent models, a small number of explicit solvent molecules treated at the quantum level, or a large number of explicit solvent molecules in a hybrid quantum mechanical/molecular mechanical (QM/MM) treated with a force field method. Implicit solvent models are the cheapest computationally but are also the least accurate by only modeling solvent as a dielectric continuum and foregoing any interactions with the solute. A small number of explicit solvent molecules are a more accurate approach and can be used alongside implicit models, but this approach fails to show information about solvation layers as a whole. The hybrid QM/MM approach is likely the most suitable when studying carbohydrates as it allows water molecules numbering in the hundreds to be included in simulations, and therefore multiple solvation shells can be included.

9.2 Structural Investigation of Carbohydrates Using ROA Spectroscopy

The first reported computational ROA study of carbohydrates was carried out by Macleod et al. (2006) who studied hydrated and isolated glucose, galactose, and

lactose in the gas phase and in aqueous solution. In experimental measurements of Raman and ROA spectra in aqueous solution at 298 K, infrared ion-dip spectroscopy was conducted at low temperatures. Gas phase calculations of the low-lying conformational structures, at the B3LYP/6-31+G* level of theory, were used to give sets of computed spectra, which in turn were used to create weighted sums in an attempt to approximate the experimental spectra recorded in solution. These calculations were compared with estimates based upon NMR measurements as well as molecular mechanics and molecular dynamics simulations (MD), giving results deemed surprisingly successful. The singly hydrated complexes of the two monosaccharides studied showed altered conformational preferences in the gas phase experiments, which were sustained in aqueous solution. These results supported the view that explicit hydration has a strong influence on aqueous phase conformations.

Luber and Reiher calculated the Raman and ROA spectra of the carbohydrate molecule 1,6-anhydro-β-D-glucopyranose (Luber and Reiher 2009b), to offer a deeper insight into an earlier published experimental ROA spectrum (Barron et al. 1991b). Boat and chair conformations of the monosaccharide were studied as well as rotamers arising from the three hydroxyl groups, giving rise to 54 conformers. These calculations exhibited the great sensitivity of ROA by showing large variations of peak intensity between rotamers. The need for solvent in calculations was treated in two ways, the implicit solvation model COSMO was used initially, and then the molecule was explicitly hydrated using several water molecules. The implicit model gave rise to minor alterations in ROA bands, but the inclusion of explicit solvent resulted in a markedly different spectrum, showing the large effect hydrogen bonding can have on the results. Final spectra were constructed by weighting individual conformers using three approaches: electronic energies, Gibbs free energies, and no weighting. The agreement with experiment was good for all types of weighting; however, it was noted that on the route to better experimental agreement, combined MD and QM/MM approaches would offer better prospects at modeling solvent effects and conformational dynamics.

Kaminsky et al. (2009) used Raman and ROA calculations coupled with MD simulations as well as the CCT transfer technique to interpret the experimental spectra of a sugar derivative, the gluconic acid anion. This linear carbohydrate exhibits large conformational flexibility due to ten dihedral angles that if carrying out mapping of the conformational space at 120° intervals would result in close to 60,000 conformers, an unfeasible number to be able to calculate a spectrum for each. To circumvent this, the authors carried out MD simulations to get a 1,000 structures and took a small sample of geometries from these simulations and calculated force fields, polarizability, and optical activity tensors at the B3LYP/6-31 + G**/CPCM level of theory. The CCT transfer technique was used with the DFT-calculated results to generate a spectrum from the MD library that reproduced most of the experimental features. It is also noted that despite a high level of spectral averaging, it is still possible to identify characteristic vibrational normal modes such as C–H and O–H bending.

One of the more recent publications in this field by Cheeseman et al. (2011) shows the future potential of the Raman and ROA calculations of carbohydrates,

by incorporating MD simulations with explicit solvation alongside QM/MM calculations. Studying the monosaccharide methyl-β-D-glucose, a selection of MD snapshots was used as the starting point for ONIOM calculations, where optimizations and force field calculations were carried out at the B3LYP/6-31G* level of theory for the monosaccharide and AMBER for the water. Calculation of Raman and ROA tensors was carried out at the HSEH1PBE/rDPS level of theory for the monosaccharide and AMBER for the water, using the two-step procedure. By incorporating the conformational dynamics and explicit solvation from the MD simulations with the quantum calculation of the ROA spectrum, excellent agreement with experiment is achieved, especially when compared to gas phase or implicit solvent calculations of the same molecule. The authors also note that this combined approach solves problems associated with the inability to model the sensitivity of ROA spectra, and it surpasses all previous approaches to include hydration in these calculations.

9.3 Structural Investigation of Carbohydrates Using Raman Spectroscopy

Due to the chiroptical nature of ROA, it makes it particularly useful in the study of carbohydrates particularly when combined with calculations, much more so then the non-chirally sensitive analogous technique Raman spectroscopy. As such there is also a lack or reported research using only Raman spectroscopy, with the only publications occurring only in the last few years.

Brizuela et al. (2012) reported one of the first examples of using computational modeling of Raman spectra to study carbohydrates in 2012, by offering a complete characterization of the Raman and FTIR spectra of the disaccharide sucrose in the solid state. They had a particular interest in structural properties including bond order, charge transfer, and topological properties of the monosaccharide rings studied using DFT calculations, natural bond orbital (NBO) analysis as well as atoms in molecules (AIM) analysis. Calculations at the B3LYP/6-31G* and B3LYP/6-311++G** levels of theory gave results that were in good agreement with experimental data and resulted in a complete assignment of the normal vibrational modes of this molecule.

A similar study to the one presented above was also carried out by Brizuela et al. (2014) on sucrose but in an aqueous medium instead of the solid phase. Self-consistent reaction field calculations were used to model the presence of solvent, and full assignment of the normal vibrational modes was achieved as well as confirming the presence of pentahydrate and dihydrate sucrose species in aqueous solution.

Quesada-Moreno et al. (2013) studied the conformational preference of the carbohydrates D-ribose and 2-deoxy-D-ribose in the aqueous and solid phase. Experimentally IR and Raman measurements were taken as well as another chiroptical technique, vibrational circular dichroism (VCD). Calculations at several levels of theory were used in this study, including MP2, B3LYP, and M06-2X, with the PCM implicit solvation model and in some calculations

a single explicit water molecule. The combination of the two approaches allowed the dominant configurations of the carbohydrates in question to be elucidated as well as discovered that for 2-deoxy-D-ribose, there are different conformer populations between solution and the solid phase.

9.4 Guidelines for Raman and ROA Calculations of Carbohydrates

In calculation of Raman and ROA spectra, several things need to be taken into account. Choice of method and basis set is important, as already shown above, but it is also important to account for the presence of all important conformers, especially when carrying out calculations on carbohydrates that exhibit high conformational flexibility.

Firstly, the structure of the molecule of choice must be constructed, and then a search of this molecule's conformational space must be undertaken. This can be carried out in several ways, such as manually exploring the angular degrees of freedom of the molecule. Although this approach is more suitable for small rigid molecules than carbohydrates, as such a better approach would be to use MD simulations, which also offers the advantage of being able to include explicit solvent molecules. The MD trajectories can then be used to obtain snapshots as starting points for Raman and ROA calculations as well as giving conformational population analysis.

Selected snapshots are used as starting points for optimization and these optimized structures are used for calculation of the force field and Raman and ROA intensities. Spectra can be plotted from these intensities using Lorentzian or Gaussian curves with ranging half-peak widths, although for most applications 10 cm^{-1} is recommended. The spectra of the individual snapshots can then be used to create a final spectrum be carrying out weighted averages, either based on Boltzmann distributions or using the population analysis from MD simulations. These computationally obtained spectra can then be compared to experimentally obtained data (Fig. 19).

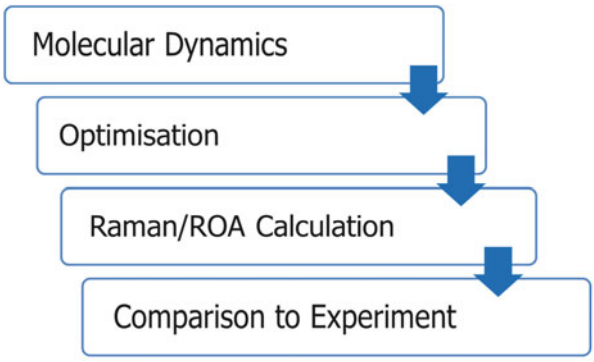

Fig. 19 Scheme showing the approach for the calculation of Raman and ROA spectra of carbohydrates

10 Conclusion

Carbohydrates present, arguably, the greatest challenge for structural biology today, not least because of their flexible natures and their heterogeneous compositions (in the case of glycoproteins) or limited complexity sequences (a significant issue for NMR studies on glycosaminoglycans). Raman spectroscopies now comprise a highly adaptable toolkit of analytical techniques that are able to provide detailed information about carbohydrates, their structures and behavior. The ability to collect such information noninvasively from environments as disparate as living cells, bioreactors, and foodstuffs can allow Raman spectroscopies to make a significant impact in glycobiology, not only in research but also in the industrial and biomedical sectors. Although this review has presented examples from a number of Raman techniques (Raman microscopy, SERS, ROA, CARS), this is not an exhaustive list, and other Raman methods are likely to prove valuable in the future. For example, the capability of tip-enhanced Raman (TERS) (Bailo and Deckert 2008) to combine the chemical sensitivity of Raman with the site specificity of atomic force microscopy has already created great interest for studies on proteins and nucleic acids (Kurouski et al. 2012; Rasmussen and Deckert 2006). The potential of TERS to provide detailed site- or region-specific information about the glycosylation patterns of individual glycoproteins would open new opportunities for researchers of these important but poorly understood systems. As we have discussed, Raman spectroscopy can be readily combined with other technologies, and hyphenated variations in the form of a single instrument package, such as Raman-mass spectrometry, are likely to prove useful in this field in the future. In parallel with technological developments, it is also likely that chemometrics will become a routine data processing step due to the already demonstrated ability of both clustering and regression algorithms to extract information about carbohydrates of any form. The many modeling tools being developed for systems biology are well suited to mining the rich detail of carbohydrate Raman spectra. Finally, the exquisite sensitivity of quantum and molecular mechanics to the vibrational modes of molecules can provide the atomic resolution level of understanding that we currently lack for most carbohydrates.

We hope that this review provides our glycobiology colleagues with an insight into how the family of Raman spectroscopies can help them understand this fascinating class of biomolecules. We encourage them to contact their local Raman experts to explore the many opportunities available for doing some new and exciting science. And to our fellow Raman spectroscopists, the future is indeed looking sweet.

References

Åkeson M, Brackmann C, Gustafsson L, Enejder A (2010) Chemical imaging of glucose by CARS microscopy. J Raman Spectrosc 41:1638–1644

Albrecht MG, Creighton JA (1977) Anomalously intense Raman spectra of pyridine at a silver electrode. J Am Chem Soc 99:5215–5217
Anker JN, Hall WP, Lyandres O, Shah NC, Zhao J, van Duyne RP (2008) Biosensing with plasmonic nanosensors. Nat Mater 7:442–453
Arboleda PH, Loppnow GR (2000) Raman spectroscopy as a discovery tool in carbohydrate chemistry. Anal Chem 72:2093–2098
Ashton LA, Pudney PDA, Blanch EW, Yakubov GA (2013) Understanding glycoprotein behaviours using Raman and Raman optical activity spectroscopies: Characterising the entanglement induced conformational changes in oligosaccharide chains of mucin. Adv Colloid Interface Sci 199:66–77
Atkins PW, Barron LD (1969) Rayleigh scattering of polarized photons by molecules. Mol Phys 16:453–466
Avetisyan A, Jensen JB, Huser T (2013) Monitoring Trehalose Uptake and Conversion by Single Bacteria using Laser Tweezers Raman Spectroscopy. Anal Chem 85:7264–7270
Bailo E, Deckert V (2008) Tip-enhanced Raman scattering. Chem Soc Rev 37:921–930
Bansil R, Yannas IV, Stanley HE (1978) Raman spectroscopy: a structural probe of glycosaminoglycans. Biochim Biophys Acta 541:535–542
Barman I, Dingari NC, Kang JW, Horowitz GL, Dasari RR, Feld MS (2012) Raman Spectroscopy-Based Sensitive and Specific Detection of Glycated Hemoglobin. Anal Chem 84:2474–2482
Barron LD, Blanch EW (2009) Raman optical activity of biological molecules. In: Matousek P, Morris M (eds) Emerging biomedical and pharmaceutical applications of Raman spectroscopy. Springer, Berlin/Heidelberg
Barron LD, Bogaard MP, Buckingham AD (1973) Raman scattering of circularly polarized light by optically active molecules. J Am Chem Soc 95:603–605
Barron LD, Gargaro AR, Wen ZQ, MacNicol DD, Butters C (1990) Vibrational Raman optical activity of cyclodextrins. Tetrahedron-Asymmetry 1:513–516
Barron LD, Gargaro AR, Hecht L, Polavarapu PL (1991a) Experimental and *ab initio* theoretical vibrational Raman optical activity of alanine. Spectrochim Acta A 47:1001–1016
Barron LD, Gargaro AR, Wen ZQ (1991b) Vibrational Raman optical activity of carbohydrates. Carbohydr Res 210:39–49
Barron LD, Gargaro AR, Hecht L, Polavarapu PL, Sugeta H (1992) Experimental and ab initio theoretical vibrational Raman optical activity of tartaric acid. Spectrochim Acta A 48:1051–1066
Barron LD, Hecht L, Blanch EW, Bell AF (2000) Solution structure and dynamics of biomolecules from Raman optical activity. Prog Biophys Mol Biol 73:1–49
Barron LD, Blanch EW, Bell AF, Syme CD, Day LA, Hecht L (2003) New insight into solution structure and dynamics of proteins, nucleic acids and viruses from Raman optical activity. In: Hicks JM (ed) Chirality: physical chirality. ACS Books, Clarendon Hills
Barron LD, Hecht L, McColl IH, Blanch EW (2004) Raman optical activity comes of age. Mol Phys 102:731–744
Bell AF, Barron LD, Hecht L (1994a) Vibrational Raman optical activity study of D-glucose. Carbohydr Res 257:11–24
Bell AF, Hecht L, Barron LD (1994b) Disaccharide Solution Stereochemistry from Vibrational Raman Optical Activity. J Am Chem Soc 116:5155–5161
Bell AF, Ford SJ, Hecht L, Wilson G, Barron LD (1994c) Vibrational Raman optical activity of glycoproteins. Int J Biol Macromol 16:277–278
Bell AF, Hecht L, Barron LD (1995) Polysaccharide vibrational Raman optical activity: Laminarin and pullulan. J Raman Spectrosc 26:1071–1074
Bell AF, Hecht L, Barron LD (1997) New evidence for conformational flexibility in cyclodextrins from vibrational Raman optical activity. Chem Eur J 3:1292–1298
Blanch EW, Hecht L, Barron LD (2003) Vibrational Raman optical activity of proteins, nucleic acids, and viruses. Methods 29:196–209

Blundell CD, DeAngelis PL, Almond A (2006) Hyaluronan: the absence of amide-carboxylate hydrogen bonds and the chain conformation in aqueous solution are incompatible with stable secondary and tertiary structure models. Biochem J 396:487–498

Bose PK, Barron LD, Polavarapu PL (1989) Ab initio and experimental vibrational Raman optical activity in (+)-(R)-methylthiirane. Chem Phys Lett 155:423–429

Bour P, Sopkova J, Bednarova L, Malon P, Keiderling TA (1997) Transfer of molecular property tensors in Cartesian coordinates: A new algorithm for simulation of vibrational spectra, J Chem Theory Comput 5:646–659

Brewster VL, Ashton L, Goodacre R (2011) Monitoring the Glycosylation Status of Proteins Using Raman Spectroscopy. Anal Chem 83:6074–6081

Brizuela AB, Bichara LC, Romano E, Yurquina A, Locatelli S, Brandan SA (2012) A complete characterization of the vibrational spectra of sucrose. Carbohydr Res 361:212–218

Brizuela AB, Castillo MV, Raschi AB, Davies L, Romano E, Brandan SA (2014) A complete assignment of the vibrational spectra of sucrose in aqueous medium based on the SQM methodology and SCRF calculations. Carbohydr Res 388:112–124

Cabassi F, Casu B, Perlin AS (1978) Infrared absorption and raman scattering of sulfate groups of heparin and related glycosaminoglycans in aqueous solution. Carbohydr Res 63:1–11

Cael JJ, Koenig JL, Blackwell J (1974) Infrared and raman spectroscopy of carbohydrates: Part IV. Identification of configuration- and conformation-sensitive modes for D-glucose by normal coordinate analysis. Carbohydr Res 32:79–91

Carmona P, Molina M (1990) Raman and infrared spectra of D-ribose and D-ribose 5-phosphat. J Raman Spectrosc 21:395–400

Cerchiaro G, Sant'Ana AC, Temperini MLA, da Costa Ferreira AM (2005) Investigations of different carbohydrate anomers in copper(II) complexes with D-glucose, D-fructose, and D-galactose by Raman and EPR spectroscopy. Carbohydr Res 340:2352–2359

Chan JW (2013) Recent advances in laser tweezers Raman spectroscopy (LTRS) for label-free analysis of single cells. J Biophotonics 6:36–48

Cheeseman JR, Frisch MJ (2011) Basis Set Dependence of Vibrational Raman and Raman Optical Activity Intensities. J Chem Theory Comput 7:3323–3334

Cheeseman JR, Shaik MS, Popelier PLA, Blanch EW (2011) Calculation of Raman Optical Activity Spectra of Methyl-β-D-Glucose Incorporating a Full Molecular Dynamics Simulation of Hydration Effects. J Am Chem Soc 133:4991–4997

Dauchez M, Derreumaux P, Lagant P, Vergoten G, Sekkal M, Legrand P (1994a) Force-field and vibrational spectra of oligosaccharides with different glycosidic linkages–Part I. Trehalose dihydrate, sophorose monohydrate and laminaribiose. Spectrochim Acta A 50A:87–104

Dauchez M, Lagant P, Derreumaux P, Vergoten G, Sekkal M, Sombret B (1994b) Force field and vibrational spectra of oligosaccharides with different glycosidic linkages–Part II. Maltose monohydrate, cellobiose and gentiobiose. Spectrochim Acta A 50A:105–118

de Oliveira LFC, Colambara R, Edwards HGM (2002) Fourier Transform Raman Spectroscopy of Honey. Appl Spectrosc 56:306–311

Delfino I, Camerlingo C, Portaccio M, Della Ventura B, Mita L, Lepore M (2011) Visible micro-Raman spectroscopy for determining glucose content in beverage industry. Food Chem 127:735–742

Diem M, Mazur A, Lenau K, Schubert J, Bird B, Milijkovic M, Krafft C, Popp J (2013) Molecular pathology via IR and Raman spectral imaging. J Biophotonics 6:855–886

Dingari NC, Horowitz GL, Kang JW, Dasari RR, Barman I (2012) Raman Spectroscopy Provides a Powerful Diagnostic Tool for Accurate Determination of Albumin Glycation. PLoS ONE 7:e32406

Dochow S, Krafft C, Neugebauer U, Bocklitz T, Henkel T, Mayer G, Albert J, Popp J (2011) Tumour cell identification by means of Raman spectroscopy in combination with optical traps and microfluidic environments. Lab Chip 13:1484–1490

Fioretto D, Comez L, Gallina ME, Morresi A, Palmieri L, Paolantoni M, Sassi P, Scarponi F (2007) Separate dynamics of solute and solvent in water–glucose solutions by depolarized light scattering. Chem Phys Lett 441:232–236

Fleischmann M, Hendra PJ, McQuillan AJ (1974) Raman spectra of pyridine adsorbed at a silver electrode. Chem Phys Lett 26:163–166

Galler K, Brautigam K, Grosse C, Popp J, Neugebauer U (2014) Making a big thing of a small cell – recent advances in single cell analysis. Analyst 139:1237–1273

Gallina ME, Sassi P, Paolantoni M, Morresi A, Cataliotti RS (2006) Vibrational Analysis of Molecular Interactions in Aqueous Glucose Solutions. Temperature and Concentration Effects. J Phys Chem B 110:8856–8864

Ghysels A, Van Neck D, Van Speybroeck V, Verstraelen T, Waroquier M (2007) Vibrational modes in partially optimized molecular systems. J Chem Phys 126:224102

Helgaker T, Ruud K, Bak KL, Jorgensen P, Olsen J (1994) Vibrational Raman optical activity calculations using London atomic orbitals. Faraday Discuss 99:165–180

Janosche R (1973) Ab initio Investigation of the IR- and Raman Activity of the Hydrogen Bond (C1HC1)- with Dfferent Environments. Theor Chim Acta 29:57–74

Jeanmaire DL, van Duyne RP (1977) Surface raman spectroelectrochemistry: Part I. Heterocyclic, aromatic, and aliphatic amines adsorbed on the anodized silver electrode. J Electroanal Chem 84:1–20

Johannessen C, Pendrill R, Widmalm G, Hecht L, Barron LD (2011) Glycan Structure of a High-Mannose Glycoprotein from Raman Optical Activity. Angew Chem Int Ed 50:5349–5351

Kačuráková M, Mathlouthi M (1996) FTIR and laser-Raman spectra of oligosaccharides in water: characterization of the glycosidic bond. Carbohydr Res 284:145–157

Kaminsky J, Kapitan J, Baumruk V, Bednarova L, Bour P (2009) Interpretation of Raman and Raman Optical Activity Spectra of a Flexible Sugar Derivative, the Gluconic Acid Anion. J Phys Chem A 113:3594–3601

Kaufmann J, Mohle K, Hofman J-G, Arnold K (1998) Molecular dynamics study of hyaluronic acid in water. J Mol Struct -theochem 422:109–121

Kitahama Y, Itoh T, Pienpinijtham P, Ekgasit S, Han XX, Ozaki Y (2012) Biological applications of SERS using functional nanoparticles. In: Hepel M, Zhong CJ (eds) Functional nanoparticles for bioanalysis, nanomedicine, and bioelectronic devices, vol 2, ACS symposium series, 1113. American Chemical Society, Washington, DC, pp 181–234

Kurouski D, Deckert-Gaudig T, Deckert V, Lednev IK (2012) Structure and Composition of Insulin Fibril Surfaces Probed by TERS. J Am Chem Soc 134:13323–13329

Larmour IA, Graham D (2011) Surface enhanced optical spectroscopies for bioanalysis. Analyst 136:3831–3853

Liegeois V, Ruud K, Champagne B (2007) An analytical derivative procedure for the calculation of vibrational Raman optical activity spectra. J Chem Phys 127:204105

Lu X, Liu Q, Benavides-Montano JA, Nicola AV, Aston DE, Rasco BA, Aguilar HC (2013) Detection of Receptor-Induced Glycoprotein Conformational Changes on Enveloped Virions by Using Confocal Micro-Raman Spectroscopy. J Virol 87:3130–3142

Luber S, Reiher M (2009a) Intensity-Carrying Modes in Raman and Raman Optical Activity Spectroscopy. ChemPhysChem 10:2049–2057

Luber S, Reiher M (2009b) Calculated Raman Optical Activity Spectra of 1,6-Anhydro-β-d-glucopyranose. J Phys Chem A 113:8268–8277

Lyandres O, Shah NC, Yonzon CR, Walsh JT, Glucksberg MR, van Duyne RP (2005) Real-Time Glucose Sensing by Surface-Enhanced Raman Spectroscopy in Bovine Plasma Facilitated by a Mixed Decanethiol/Mercaptohexanol Partition Layer. Anal Chem 77:6134–6139

Ma K, Yuen JM, Shah NC, Walsh JT, Glucksberg MR, van Duyne RP (2011) In Vivo, Transcutaneous Glucose Sensing Using Surface-Enhanced Spatially Offset Raman Spectroscopy: Multiple Rats, Improved Hypoglycemic Accuracy, Low Incident Power, and Continuous Monitoring for Greater than 17 Days. Anal Chem 83:9146–9152

Macleod NA, Johannessen C, Hecht L, Barron LD, Simons JP (2006) From the gas phase to aqueous solution: Vibrational spectroscopy, Raman optical activity and conformational structure of carbohydrates. Int J Mass Spectrom 253:193–200

Mathlouthi M, Koenig JL (1986) Vibrational spectra of carbohydrates. Adv Carbohydr Chem Biochem 44:7–89

Mathlouthi M, Seuvre AM, Koenig JL (1983) F.T.-I.R. and laser-raman spectra of d-ribose and 2-deoxy-d-erythro-pentose ("2-deoxy-d-ribose"). Carbohydr Res 122:31–47

Matsuhiro B, Osorio-Román IO, Torres R (2012) Vibrational spectroscopy characterization and anticoagulant activity of a sulfated polysaccharide from sea cucumber Athyonidium chilensis. Carbohydr Polym 88:959–965

McNay G, Eustace D, Smith WE, Faulds K, Graham D (2011) Surface-Enhanced Raman Scattering (SERS) and Surface-Enhanced Resonance Raman Scattering (SERRS): A Review of Applications. Appl Spectrosc 65:825–837

Mensch C, Pendrill R, Widmalm G, Johannessen C (2014) Studying the Glycan Moiety of RNase B by Means of Raman and Raman Optical Activity. ChemPhysChem 15:2252–2254

Mrozek MF, Weaver MJ (2002) Detection and Identification of Aqueous Saccharides by Using Surface-Enhanced Raman Spectroscopy. Anal Chem 74:4069–4075

Mrozek MF, Zhang D, Ben-Amotz D (2004) Oligosaccharide identification and mixture quantification using Raman spectroscopy and chemometric analysis. Carbohydr Res 339:141–145

Ortiz C, Zhang D, Xie Y, Ribbe AE, Ben-Amotz D (2006) Validation of the drop coating deposition Raman method for protein analysis. Anal Biochem 353:157–166

Ostovar pour S, Bell SEJ, Blanch EW (2011) Use of a hydrogel polymer for reproducible surface enhanced Raman optical activity (SEROA). Chem Commun 47:4754–4756

Paolantoni M, Sassi P, Morresi A, Santini S (2007) Hydrogen bond dynamics and water structure in glucose-water solutions by depolarized Rayleigh scattering and low-frequency Raman spectroscopy. J Chem Phys 127:024504

Pecul M, Rizzo A (2003) Raman optical activity spectra: basis set and electron correlation effects. Mol Phys 101:2073–2081

Perticaroli S, Sassi P, Morresi A, Paolantoni M (2008) Low-wavenumber Raman scattering from aqueous solutions of carbohydrates. J Raman Spectrosc 39:227–232

Polavarapu PL (1990) Ab initio vibrational Raman and Raman optical activity spectra. J Phys Chem 94:8106–8112

Quesada-Moreno MM, Azofra LM, Aviles-Moreno JR, Alkorta I, Elguero J, Lopez-Gonzalez JJ (2013) Conformational Preference and Chiroptical Response of Carbohydrates D-Ribose and 2-Deoxy-D-ribose in Aqueous and Solid Phases. J Phys Chem B 117:14599–14614

Rasmussen A, Deckert V (2006) Surface- and tip-enhanced Raman scattering of DNA components. J Raman Spectrosc 37:311–317

Reiher M, Liegeois V, Ruud K (2005) Basis Set and Density Functional Dependence of Vibrational Raman Optical Activity Calculations. J Phys Chem A 109:7567–7574

Ringe E, Sharma B, Henry A, Marks LD, van Duyne RP (2013) Single nanoparticle plasmonics. Phys Chem Chem Phys 15:4110–4129

Rudd TR, Hussain R, Siligardi G, Yates EA (2010) Raman and Raman optical activity of glycosaminoglycans. Chem Commun 46:4124–4126

Ruud K, Thorvaldsen AJ (2009) Theoretical approaches to the calculation of Raman optical activity spectra. Chirality 21:E54–E67

Ruud K, Helgaker T, Bour P (2002) Gauge-Origin Independent Density-Functional Theory Calculations of Vibrational Raman Optical Activity. J Phys Chem A 106:7448–7455

Schafer-Peltier KE, Haynes CL, Glucksberg MR, van Duyne RP (2003) Toward a Glucose Biosensor Based on Surface-Enhanced Raman Scattering. J Am Chem Soc 125:588–593

Schlucker S (2009) SERS Microscopy: Nanoparticle Probes and Biomedical Applications. ChemPhysChem 10:1344–1354

Schlucker S (2014) Surface-Enhanced Raman Spectroscopy: Concepts and Chemical Applications. Angew Chem Int J 53:4756–4795

Smyth E, Syme CD, Blanch EW, Hecht L, Vasak M, Barron LD (2001) Solution structure of native proteins with irregular folds from Raman optical activity. Biopolymers 58:138–151

Soderholm S, Roos YH, Meinander N, Hotokka M (1999) Raman spectra of fructose and glucose in the amorphous and crystalline states. J Raman Spectrosc 30:1009–1018

Vangala K, Yanney M, Hsiao C-T, Wu WW, Shen R-F, Zou S, Sygula A, Zhang D (2010) Sensitive Carbohydrate Detection Using Surface Enhanced Raman Tagging. Anal Chem 82:10164–10171

Wang L, Mizaikoff B, Kranz C (2009) Quantification of Sugar Mixtures with Near-Infrared Raman Spectroscopy and Multivariate Data Analysis. A Quantitative Analysis Laboratory Experiment. J Chem Educ 86:1322–1325

Wells HA Jr, Atalla RH (1990) An investigation of the vibrational spectra of glucose, galactose and mannose. J Mol Struct 224:385–424

Wen ZQ, Barron LD, Hecht L (1993) Vibrational Raman optical activity of monosaccharides. J Am Chem Soc 115:285–292

Xu H, Li Q, Wang LH, He Y, Shi JY, Tang B, Fan CH (2014) Nanoscale optical probes for cellular imaging. Chem Soc Rev 43:2650–2661

Yaffe NR, Almond A, Blanch EW (2010) A New Route to Carbohydrate Secondary and Tertiary Structure Using Raman Spectroscopy and Raman Optical Activity. J Am Chem Soc 132:10654–10655

Yamamoto S, Bour P (2011) On the limited precision of transfer of molecular optical activity tensors. Collect Czechoslov Chem Commun 76:567–583

Yamamoto YS, Ishikawa M, Ozaki Y, Itoh T (2014) Fundamental studies on enhancement and blinking mechanism of surface-enhanced Raman scattering (SERS) and basic applications of SERS biological sensing. Front Phys 9:31–46

Yuen JM, Shah NC, Walsh JT, Glucksberg MR, van Duyne RP (2010) Transcutaneous Glucose Sensing by Surface-Enhanced Spatially Offset Raman Spectroscopy in a Rat Model. Anal Chem 82:8382–8385

Zhu FJ, Isaacs NW, Hecht L, Barron LD (2005) Polypeptide and Carbohydrate Structure of an Intact Glycoprotein from Raman Optical Activity. J Am Chem Soc 127:6142–6143

Zuber G, Hug W (2004) Rarefied Basis Sets for the Calculation of Optical Tensors. 1. The Importance of Gradients on Hydrogen Atoms for the Raman Scattering Tensor. J Phys Chem A 108:2108–2118